EXPERIMENTAL CELL RESEARCH 314 (2008) 2334–2351

available at www.sciencedirect.com

ScienceDirect

www.elsevier.com/locate/yexcr

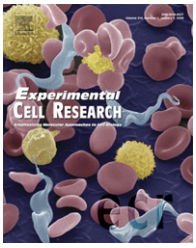

Research Article

Osteoactivin, an anabolic factor that regulates osteoblast differentiation and function

Samir M. Abdelmagid[a], *Mary F. Barbe*[a,b], *Mario C. Rico*[a,1], *Sibel Salihoglu*[a], *Israel Arango-Hisijara*[a], *Abdul Hafez Selim*[a], *Michael G. Anderson*[c], *Thomas A. Owen*[a], *Steven N. Popoff*[a], *Fayez F. Safadi*[a,*]

[a]*Department of Anatomy and Cell Biology, Temple University, School of Medicine, 3400 North Broad Street, Philadelphia, PA 19140, USA*
[b]*Department of Physical Therapy, Temple University, Philadelphia, PA, USA*
[c]*Department of Molecular Physiology and Biophysics, University of Iowa, Iowa, IA, USA*

ARTICLE INFORMATION

Article Chronology:
Received 4 December 2007
Revised version received
2 February 2008
Accepted 8 February 2008
Available online 10 March 2008

Keywords:
Osteoactivin
Osteoblast differentiation
Matrix mineralization

ABSTRACT

Osteoactivin (OA) is a novel glycoprotein that is highly expressed during osteoblast differentiation. Using Western blot analysis, our data show that OA protein has two isoforms, one is transmembranous and the other is secreted into the conditioned medium of primary osteoblasts cultures. Fractionation of osteoblast cell compartments showed that the mature, glycosylated OA isoform of 115 kDa is found in the membranous fraction. Both OA isoforms (secreted and transmembrane) are found in the cytoplasmic fraction of osteoblasts. Overexpression of EGFP-tagged OA in osteoblasts showed that OA protein accumulates into vesicles for transportation to the cell membrane. We examined OA protein production in primary osteoblast cultures and found that OA is maximally expressed during the third week of culture (last stage of osteoblast differentiation). Glycosylation studies showed that OA isoform of 115 kDa is highly glycosylated. We also showed that retinoic acid (RA) stimulates the mannosylation of OA protein. In contrast, tunicamycin (TM) strongly inhibited N-glycans incorporation into OA protein. The functional role of the secreted OA isoform was revealed when cultures treated with anti-OA antibody, showed decreased osteoblast differentiation compared to untreated control cultures. Gain-of-function in osteoblasts using the pBABE viral system showed that OA overexpression in osteoblast stimulated their differentiation and function. The availability of a naturally occurring mutant mouse with a truncated OA protein provided further evidence that OA is an important factor for terminal osteoblast differentiation and mineralization. Using bone marrow mesenchymal cells derived from OA mutant and wild-type mice and testing their ability to differentiate into osteoblasts showed that differentiation of OA mutant osteoblasts was significantly reduced compared to wild-type osteoblasts. Collectively, our data suggest that OA acts as a positive regulator of osteoblastogenesis.

* *Corresponding author*. Fax: +1 215 707 2966.
E-mail addresses: fsafadi@temple.edu, fayezsafadi@gmail.com (F.F. Safadi).
[1] Current address: Department of Physiology, Temple University School of Medicine, Philadelphia , PA 19140, USA.

0014-4827/$ – see front matter © 2008 Elsevier Inc. All rights reserved.
doi:10.1016/j.yexcr.2008.02.006

Introduction

The initial identification of osteoactivin (OA) emerged from studies using an animal model of osteopetrosis [1]. Other groups have also identified the same protein in different species, and have designated different names, such as glycoprotein nmb (gpnmb) in melanoma cell lines [2–6], and melanocytes [7,8], dendritic cell heparan sulfate proteoglycan integrin dependent ligand (DC-HIL) in dendritic cells [9,10] and human hematopoietic growth factor inducible neurokinin (HGFIN) in tumor cells [11]. OA has high homology to Pmel-17, a melanosomal protein that is well characterized in melanocytes and plays a role in melanin fibril formation [12–19]. These similarities suggest that OA may belong to the same gene family as Pmel-17. The OA protein is a type I transmembrane protein with two isoforms, one is membranous and the other is secreted [1,9,10,20–23].

Recent reports demonstrated the cellular functions of OA showing that OA has the ability to regulate cell proliferation, adhesion, differentiation and synthesis of extracellular matrix (ECM) proteins in various cell types, in normal and pathological conditions [1–3,6–10,20–31]. Some animal models have been generated to demonstrate OA function in different tissues. OA transgenic (Tg) mice that overexpress OA under the CMV promoter showed increased muscle mass and enhanced expression of MMP-3 and MMP-9 in fibroblasts from denervated skeletal muscle model [30]. Another study in transgenic rats that overexpress OA in liver cells showed that OA attenuates the development of hepatic fibrosis [29]. The most exciting animal model is the natural mutation of OA gene in the mouse causing a premature stop codon that results in the generation of a truncated OA protein [7,8,32,33]. These mice develop an eye phenotype with iris pigmentary dispersion and iris stromal atrophy. They also have increased macrophage function [34]. With the development of these animal models, there has been an increased focus on OA and its effects on different cellular and pathological processes. However, there is still a great deal of work that needs to be done to determine the functions of osteoactivin and its mechanism(s) of action.

In bone and using the *osteopetrotic* (*op*) rat as a model to examine differential gene expression in bone from normal and osteopetrotic rats, we discovered that OA mRNA expression was significantly increased in osteopetrotic bone [1]. Our group was the first to report the expression and function of OA in bone. Previously, we demonstrated that OA mRNA and protein are expressed by human and rodent osteoblasts and its expression exhibited a temporal pattern during osteoblast differentiation reaching highest levels during the later stages of matrix maturation and mineralization [1,20,22,23].

OA and Pmel-17 are heavily glycosylated proteins with O- and N-linked glycans [20,35]. Glycosylation of proteins plays a crucial role in cell differentiation and function [36]. Understanding the mechanism mediating OA protein processing and glycosylation will shed light on its mechanism(s) of action. While processing and regulation of Pmel-17 in melanocytes has been well described by different laboratories [35,37,38]. There are no reports that characterize OA processing and secretion by osteoblasts. Here we provide evidence that OA is synthesized and secreted by osteoblasts during differentiation. There are two isoforms of OA, one is transmembrane and the other is secreted and the secreted isoform is heavily glycosylated and plays a role in osteoblast differentiation and function. We also present evidence that OA glycosylation is regulated by retinoic acid and tunicamycin. These data will help to elucidate the mechanism/s of action of OA protein in osteoblast differentiation and function.

Materials and methods

Bioinformatic analysis

The amino acid sequence for OA protein was obtained in FASTA format from SWISSPORT database (http://us.expasy.org/sprot/). Signal peptide sequence of OA protein was analyzed by SignalP server. Trans-membrane hydrophobic sequence of OA protein was analyzed by TransMemb server. O-glycosylation sites on OA protein were analyzed by net OGlyc server. All servers were provided by the Center for Biological Sequence Analysis database.

Osteoactivin mutant mice

Mice mutant for osteoactivin (DBA/2J) were purchased from Jackson laboratory. Wild type mice (DBA) were purchased from Teconic laboratory. Mutant and wild-type mice were bred and maintained at Temple University School of Medicine Central Animal Barrier Facility accordering to the guidelines of the Institutional Animal Care and Use Committee (IACUC).

Generation of OA antibody

Anti-OA antibody (OA-551) was raised against the peptide sequence of amino acids 551 to 568 and anti-OA antibody (OA-35) was raised against the peptide sequence of amino acids 35–51. Both peptides were selected because of its potential antigenicity and were screened against the protein database to ensure lack of homology with other sequences. Chickens were immunized, and the precipitated crude IgY was purified by affinity chromatography on Sepharose 4B derivatised with the immunizing peptide (Cambridge Research Biochemicals, Stockton-Tees, UK).

Primary osteoblast and bone marrow cultures

Primary osteoblasts were isolated and cultured as described previously [23]. Briefly, Neonatal rat pups were decapitated; the calvaria were harvested and placed into a Petri dish with 20 ml isolation media. The calveria were cut into smaller pieces and placed into a siliconized flask with digestion media. Cells were digested three times in a medium containing collagenase-P as described previously [1,23]. The supernatants were collected from all 3 digestions and centrifuged. The cell pellets were resolubilised into 5 ml of fresh washing media. Cells were then plated in a 100 mm Petri dish at a density of 500,000 cells with 10 ml initial plating medium and incubated at 37 °C with 5% CO_2. Differentiating factors (10 mM β glycerol phosphate + 50 μg/ml ascorbic acid) were added on day 3 and every time culture media was changed.

For osteoblast differentiation using bone marrow mesenchymal stem cells, 8 weeks old osteoactivin mutant and wild-type mice were used for harvesting the bone marrow from their femora and tibae. Bone marrow cells were filtered, counted

and plated overnight. Adherent stem cells were cultured for different time points in osteogenic media containing αMEM supplemented with 10% FBS, 10^{-8} M dexamethasone, 70 ng/ml L-ascorbic acid and 8 mM β-glycerol phosphate.

Generation of OA-pBABE stable MC3T3-E1 cell line

MC3T3-E1 murine calverial osteoblast-like cell line (subclone 14) was obtained from Dr. Franceschi, (University of Michigan). A pBabe viral vector containing OA cDNA was provided to us from Dr. Jeremy Rich at Duke University. For the generation of OA-pBabe viral vector please refer to [21]. For propagating the OA-pBabe viral vector, OA-pBabe retroviral vector or control pBabe (empty vector) were co-transfected with a PCL10-A1 packaging vector, into subconfluent 293 HEK (human embryonic kidney) cell line using the calcium chloride method [21]. Virus-containing supernatant was harvested after 48 h and was used to infect MC3T3-E1 cells. For generation of stable virus producing cell line, infected MC3T3-E1 cells were splitted and selected by replacing the medium with Bleomycin antibiotic (500 μg/ml) containing medium. The medium was changed after 72 h with continued selection. After 5 days, the antibiotic resistant colonies were selected and used for further cultures.

Co-localization of OA and endoplasmic reticulum (ER) in primary osteoblasts

Primary osteoblasts were cultured in chamber slides at a density of 5000 cells/well. On the second day of culture, cells were fixed, washed and double labeled with OA using anti-OA antibody and 3,3′-dihexyloxacarbocyanine iodide ($DiOC_6(3)$, a green-fluorescent, lipophilic dye (Invitrogen) that stains the ER, followed by anti-chicken-Cy3-conjugated secondary antibody. Cells were washed with PBS and visualized using E600 Nikon fluorescent microscope.

Transfection of EGFP-tagged-OA and cellular labeling

Primary osteoblasts were cultured in 2-chamber slides at a density of 5000 cells/well. On the second day of culture, cells were transfected with either GFP empty vector or GFP-tagged CMV-OA construct using Lipofectamine 2000 (Invitrogen, Carlsbad, CA). On day 3, cultured cells were fixed with 4% paraformaldehyde in 1× PBS for 15 min at R.T. Cells were washed 3 times (10 min each) with 1× PBS, and cover slipped using 80% glycerol in PBS. Slides were then examined using confocal laser scanning microscope. For co-localization of GFP-OA protein in the plasma membrane, cells were transfected as above and the cell membrane was labeled using lipophilic tracer DiD (Molecular Probes, Eugene, OR) in a 5 μM working concentration. Cells were incubated with DiD dye for 5 min at 37 °C and then for an additional 15 min at 4 °C, then washed with 1× PBS. Slides were cover slipped using 80% glycerol in PBS. Slides were examined using confocal laser scanning microscope.

RNA isolation

RNA was isolated as described previously [23]. Briefly, cell cultures were harvested then homogenized in Trizol, separated into organic and aqueous layer by chloroform, and RNA was recovered from the aqueous layer by isopropyl alcohol precipitation. Pellets were washed with 70% ethanol and concentration of RNA was calculated using spectrophotometer. For the evaluation of RNA integrity, 1 μg total RNA was run on formaldehyde gel and stained with Ethedium bromide.

RT and quantitative (q)PCR analysis

RT-PCR analysis for OA and G3PDH was performed as previously [23]. Briefly, 2 μg of total RNA were reverse transcribed to cDNA. Two microliters of the generated cDNA was amplified in 50 μl of qPCR reaction mixture. The primers for rat OA were sense; 5′-CCAGAAGAATGACCGGAACTCG-3′ and antisense 5′-CAGGCTTCCGTGGTAGTGG-3′ and the primers for rat G3PDH were sense; 5′-ACCACAGTCCATGCCATCAC-3′ and antisense 5′-TCCACCACCCTGTTGCTGTA-3′. Q-PCR was performed on ABI PRISM 7700 using the SYBR Green method. OA values were quantified using the equation ($-\Delta\Delta C_T$); C_T = threshold cycle.

Fractionation of cellular compartments

Different cellular compartments were fractionated using membrane protein extraction reagent kit (Pierce, Rockford, IL). Briefly, cells were harvested from primary osteoblasts cultured for 3 weeks, and centrifuged at 850 ×*g* for 2 min; the cell pellet was then washed in PBS. Next, 150 μl of reagent A (detergent) was added to the cell pellet with pipetting up and down to ensure a homogenous cell suspension. The mixture was then incubated for 10 min at R.T. with occasional vortexing. Next, 450 μl of diluted reagent C (a detergent diluted according to manufacturer's protocol) was added to the cell lysate and left on ice for 30 min with vortexing every 5 min. The cell lysate was centrifuged at 10,000 ×*g* for 3 min at 4 °C. The supernatant was transferred to a new tube and incubated for 10 min at 37 °C to separate the hydrophobic integral membrane proteins from the hydrophilic proteins through phase partitioning. The Mem-PER Kit was found to be highly efficient in the extraction of integral membrane proteins containing one or two transmembrane spanning domains and results were found consistent among different cell lines [39].

For isolation of the nuclear and cytoplasmic fraction, 20 μl of packed cell volume was isolated by centrifugation at 500 ×*g* for 2 min. The supernatant was discarded, leaving the cell pellet as dry as possible. Two hundreds μl of ice-cold CER I was added to the cell pellet and vortexed vigorously on the highest setting for 15 s to fully re-suspend the cell pellet. The cell pellet was then incubated on ice for 10 min. Eleven μl of ice-cold CER II was added to the tube and vortexed for 5 s before incubation on ice for 1 min. The tube was centrifuged at 16,000 ×*g* for 5 min and the supernatant (cytoplasmic extract) fraction was transferred to a new tube on ice. The insoluble pellet fraction was re-suspended in 100 μl of ice-cold NER. The tube was incubated on ice and vortexed every 10 min, for a total of 40 min. The tube was centrifuged at 16,000 ×*g* for 10 min before transferring the supernatant (nuclear extract) fraction to a new tube on ice. Pierce NE-PER reagents enable preparation of functional cytoplasmic and nuclear fractions from the same set of cells and the extraction process is gentle yet efficient in

terms of high protein yield and minimal (<10%) cross-contamination between the fractions [40].

Treatment with retinoic acid and tunicamycin

Primary osteoblasts were cultured in 6-well plates at a density of 50,000 cells/well, rinsed with Hank's medium, and treated with 10^{-6} M all-trans-retinoic acid (RA) (Sigma-Aldrich, St. Louis, MO) in the presence or absence of 1 μg/ml of tunicamycin (TM) (A.G. Scientific, San Deigo, CA) or TM alone for 24 h. Untreated cultures served as controls. Cultures were terminated on day 14 and 21, depending on the experimental protocol. OA protein expression was then assessed using Western blot analysis.

Incorporation of radiolabeled sugar molecules into OA protein

Primary osteoblasts were cultured in 6-well plates at a density of 50,000 cells/well for 5 days. Cells were treated with 10^{-6} M of RA in the presence or absence of 1 μg/ml of TM. Untreated cultures were served as controls. After 24 h, cells were washed with PBS and incubated with serum free medium containing ^{14}C mannose (1 μCi/ml) for 12 h at 37 °C. Incorporation was determined by cooling the plates to 0 °C, removing the medium, and washing twice with cold PBS. OA protein was immunoprecipitated and radioactivity incorporated was counted in a liquid scintillation counter. For de-glycosylation experiments, the OA immunoprecipitated beads were treated with PNGase for 3 h at 37 °C and the release of ^{14}C mannose into the supernatant was determined in a liquid scintillation counter.

Protein isolation

Total protein was isolated as described previously [23]. Briefly, osteoblast cultures terminated at different time points, based on the experimental strategies, were trypsinized with 0.25% trypsin and centrifuged for 10 min. Cells were lysed in RIPA buffer and protein concentration was measured using bicinchoninic acid (BCA) protein assay.

Protein de-glycosylation

Twenty μg of total protein isolated from 21 day primary osteoblast cultures was treated with enzymatic carborelease kit (QA-bio, Rockford, IL) to free *N*- and *O*-linked sugar groups. Total protein sample was mixed with 10 μl reaction buffer in 35 μl distilled water. Denaturation buffer (2.5 μl) was added to the protein sample and mixed gently, boiled at 100 °C for 5 min and chilled on ice. 2 μl of each enzyme (PNGase-F, sialidase, β-galactosidase, glucosaminidase, and *O*-glycosidase) was added to the protein sample and incubated for 3 h in water bath at 37 °C.

Immunoprecipitation

Fifty μg of total proteins isolated from primary osteoblast cultures were immunoprecipitated using an immunoprecipitation kit (Roche Diagnostic, Corp., IN) to isolate OA proteins. 25 μl of agarose A/G beads were added to each protein sample and incubated overnight at 4 °C. Beads were sedimented by centrifugation at 12000 ×*g* for 20 s then the supernatant was transferred to fresh tube for immunoprecipitation according to the manufacturer's protocol. Twenty five μl of gel loading buffer was added to each sample; proteins were denatured by heating to 100 °C for 5 min and analyzed by SDS gel electrophoresis.

Western blot analysis

Protein was isolated and subjected to SDS-PAGE as described previously [23]. Briefly, proteins isolated from primary cultures were mixed with denature buffer and heated at 100 °C for 5 min. Samples were subjected to 10% SDS-PAGE in 1× TGS for one h. Gel was then transferred to PVDF membrane by semi-dry transfer apparatus (Biorad, Hercules, CA) for one h. The blot was incubated in blocking buffer (0.5% BSA and skim milk in PBS) for one h then primary antibody was added to blocking buffer overnight at 4 °C. The blot was washed 5 times in 1× TTBS 5 min each then incubated with HRP-conjugated secondary antibody, for one h. The blot was washed again in TTBS for 5 times and the signals were developed using ECL kit and detected on XL-exposure films.

Staining of sugar molecules within OA protein

For the evaluation of sugar molecules incorporated within OA protein, immunoprecipitated OA protein was subjected to SDS-PAGE. Gel was then stained using Pro-Q Emerald Glycoprotein Gel Stain kit (Molecular Probes, Eugene, OR). The gel was incubated in 100 ml of fix solution (50% methanol and 5% acetic acid in dH_2O) at R.T. for 45 min to wash out SDS. The gel was washed in 100 ml of wash solution (3% glacial acetic acid in dH_2O) with gentle agitation at R.T. for 20 min. The gel was then incubated in 25 ml of oxidizing solution (3% acetic acid and 1% periodic acid) with gentle agitation for 30 min. The gel was washed again in 100 ml of wash solution for 20 min then incubated with 25 ml of the pro-Q emerald solution diluted 1:50 in staining buffer with gentle agitation for 90 min. The signals were detected via Alpha Imager apparatus with ultraviolet light.

Alkaline phosphatase (ALP) activity measurement

ALP activity was measured as described previously [20]. Briefly, cell layers of 14 day old culture were treated with TZM buffer for 30 min. Aliquots were mixed with *p*-nitrophenol substrate in 10× methylating triazene temozolomide (TZM) buffer. ALP activity results were normalized to the total protein content.

Alkaline phosphatase histochemistry

Primary cultures were stained for Alkaline Phosphatase (ALP) as described previously [23]. Briefly, ALP staining was performed on cultures at day 14 using ALP staining kit (Sigma). Cells were counterstained with hematoxylin and allowed to air dry before evaluating with inverted microscope.

Osteocalcin measurement

Osteocalcin concentration was measured using sandwich ELISA kits as described previously [20]. Briefly, cell layers and conditioned media of 21 day old cultures and standards were incubated in ELISA plates. After incubation with peroxidase-

conjugated secondary antibody for 1 h, TMB substrate was added for 30 min and absorbance was read at 450 nm using ELISA reader. Osteocalcin values (ng/ml) were normalized to the total protein content.

Calcium measurement

Calcium concentration was determined as described previously [20]. Briefly, cell layers of 21 day old cultures were lyzed with 0.5 N HCl. Aliquots were mixed with calcium binding reagent and read at 575 nm using spectrophotometer. Calcium values were calculated from the standard curve.

von Kossa staining of mineralized nodules

Primary cultures were stained for mineralization as described previously [23]. Briefly, von Kossa staining was used to stain osteoblast mineralized nodules on day 21. Cells were counterstained with 1% fast green then rinsed with dH_2O and allowed to air dry. Cells were then evaluated with TE300 inverted microscope.

MTT-cell viability assay

Cell viability assay was performed as described previously [23]. Briefly, MTT substrate was added on cultured osteoblasts in 24-well plate (100 μl/well) and incubated for 4 h. Solubilizer was added (250 μl/well) overnight. Samples were read in 96-well plate on ELISA reader at 570 nm.

Image analysis

Pictures were analyzed as described previously [23]. Briefly, pictures were obtained from different fields and images were analyzed using BioquantOsteo software. The size of the nodules was computed using the area measurement option of the program. Nodule mineralization was computed using the videocount area array option. Percent area fractions of alkaline phosphatase or von Kossa staining were calculated by dividing the videocount area containing pixels at or above the threshold by the videocount area of total number of pixels in the entire field, and multiplying by 100. This determination was made at 4 different locations per well, 4 wells per group.

Statistical analysis

For multiple group comparison, analysis of variance (ANOVA) was used to evaluate the effect of one variable on multiple independent groups. In the event of a significant group effect, individual pairs of means were compared using Newman–Keuls post hoc test. A p value ≤ 0.05 was considered statistically significant. Group means + standard error of the mean (SEM) were plotted in graphs.

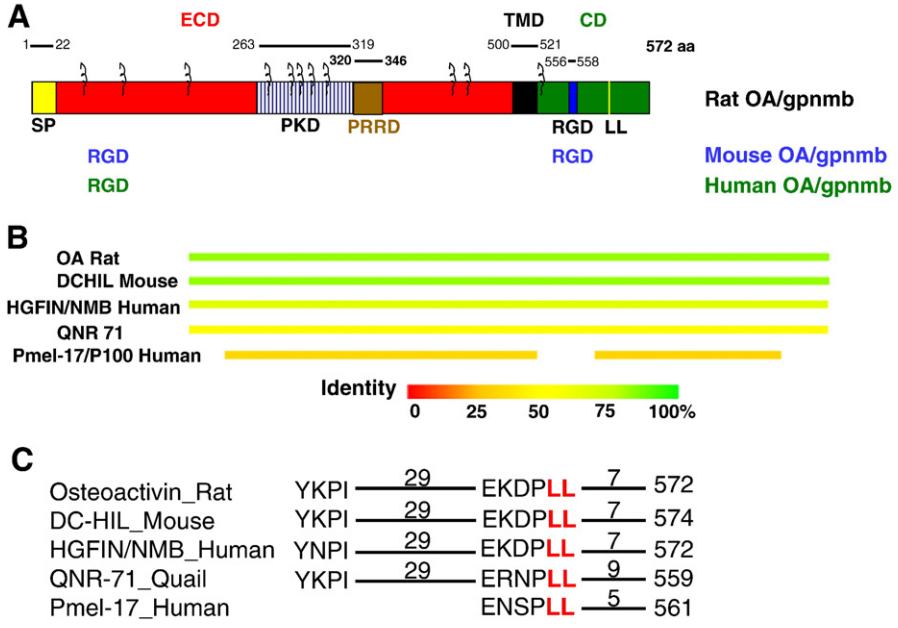

Fig. 1 – Primary structure of osteoactivin protein and its homology to other family members. (A) Schematic diagram of the primary structure of osteoactivin drawn to scale. The protein consists of three main parts, the extracellular domain (ECD), the transmembrane domain (TMD) and the cytoplasmic domain (CD). Numbers correspond to amino acid position. SP, signal peptide; PKD, polycystic kidney disease domain; PRRD, proline rich repeat domain; LL, dileucine sorting sequence; RGD, integrin binding domain. (B) High homology of rat OA to mouse DC-HIL, human HGFIN, human NMB, quail QNR-71 and human PMEL17. Percent of homology is represented by different colors in the identity bar. DC-HIL, denderitic cell heparan sulfate proteoglycan integrin dependent ligand; HGFIN, hematopoietic growth factor inducible neurokinin; NMB, non-melanoma B; QNR71, quail neuroretina; Pmel-17/gP100, melanocyte specific protein. (C) Sequence alignment of the cytoplasmic domain of integral membrane proteins targeted to vacuoles or melanosomes. Red labeled amino acids are the di-leucine- and tyrosine-based sorting signals in the indicated proteins. The indicated numbers reflect the number of amino acids between two signals.

Results

Characterization of OA protein sequence and its homology to different family members

Osteoactivin (OA), also known as glycoprotein nmb (gpnmb), is a type I transmembrane glycoprotein that consists of at least three different domains; an N-terminal domain with a signal peptide, a polycystic kidney disease domain (PKD) domain, and a transmembrane domain (TRD) (Fig. 1A). The protein also contains an Arg–Gly–Asp (RGD) cell attachment domain, for integrin-mediated cell attachment and spreading [41]. As shown in Fig. 1B, the rat OA protein shares 88% homology with mouse osteoactivin, also known as dendritic cell heparan sulfate proteoglycan integrin dependent ligand (DC-HIL,); 77% homology with human hematopoietic growth factor inducible neurokinin (HGFIN) and human nmb; and 65% and 60% homology, with quail neuroretina protein (QNR71) and human Pmel-17/gP100 melanocyte specific protein, respectively. All of these proteins contain all of the domains described for OA (Fig. 1A). OA also contains a sorting signal sequence in close proximity to the C-terminal domain. This signal sequence contains di-leucine amino acids with a consensus sequence of EXXPLL, and is located 7 amino acids away from the C-terminal end of the protein. There is another signal sequence located 29 amino acids upstream of the sorting sequence, and this sequence has been suggested to play a role in protein sorting through the rough endoplasmic reticulum and the Golgi complex [42]. This signal sequence contains one tyrosine with a consensus sequence of YXPI (Fig. 1C).

Bioinformatic analysis of the amino acid sequence of the OA protein showed that the first 22 amino acids constitute a signal peptide [1]. Further analysis showed that the OA protein has a transmembrane hydrophobic amino acid sequence from 499 to 521 (Supplemental Figure 1A). Analysis of the secondary structure of the OA protein sequence demonstrated that OA has an alpha helical structure from 500 to 521 (Supplemental Figure 1B). Analysis of the native/immature MW of OA showed that OA protein has a predicted MW of 63.8 kDa [1] and has a potential 11 *N*-linked [20] and 19 *O*-linked glycosylation sites (Supplemental Figure 1C). Collectively, these data suggest that OA protein is highly glycosylated and has two isoforms, secreted and transmembrane.

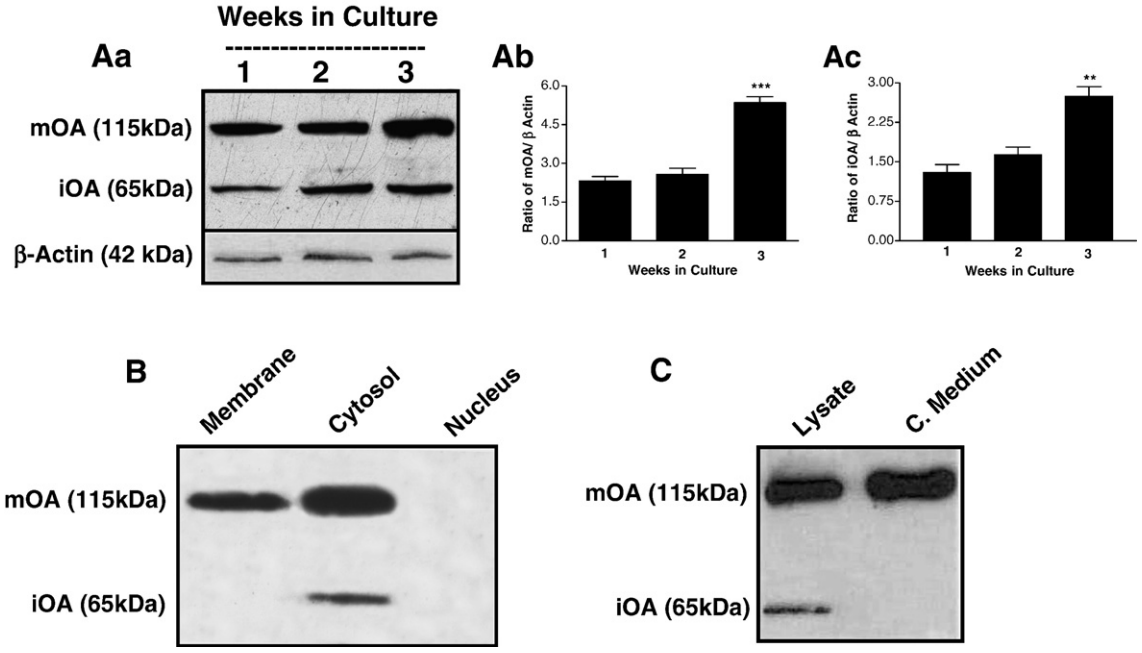

Fig. 2 – Osteoactivin expression during osteoblast differentiation. Primary rat osteoblasts were cultured and terminated after 1, 2 or 3 weeks of culture. (Aa) Immunoblot showed that the glycosylated, mature OA isoform (115 kDa) was expressed at higher levels than the immature OA isoform (65 kDa) after 3 weeks in culture. β actin was used as a loading control. (Ab and Ac) Densitometry of 3 immunoblots quantifying percent of the mature/glycosylated (115 kDa) (Ab), or the immature (65 kDa) isoforms (Ac) of OA protein as a ratio of β actin. Bars represent mean + SEM. ** = $p < 0.01$, *** = $p < 0.001$ when compared to first week of culture. (B and C) Localization of OA isoforms in osteoblasts. Primary osteoblasts were cultured for 3 weeks and cell lysates were fractionated. (B) Immunoblot showed that the cytoplasmic compartment (cytosol) contains both the glycosylated/mature (mOA) isoform of 115 kDa and the native (immature) (iOA) isoform of 65 kDa. The membranous fraction (membrane) showed expression of the only glycosylated/mature OA isoform. There was no expression of either OA isoforms in the nuclear fraction (nucleus). (C) Primary osteoblasts were cultured for 3 weeks, and then switched to serum free medium for 24 h prior termination. Immunoblot showed that the mature highly glycosylated mOA isoform of 115 kDa is secreted into the conditioned medium (C. Medium). The osteoblast cell lysate contains both glycosylated/mature (mOA) and native/immature (iOA) isoforms of OA protein.

OA expression during osteoblast differentiation in culture

Expression of the endogenous OA protein isoforms was compared at the 3 stages of osteoblast development in culture (cell proliferation between days 3–7, matrix maturation between days 7–14, and matrix mineralization between days 14–21). Western blot analysis showed that OA was detected as two distinctly different molecular weight protein bands, one reflecting the native, immature protein at 65 kDa and the other reflecting a post-translationally modified isoform of the protein at 115 kDa (Fig. 2A). The temporal pattern of OA expression during osteoblast differentiation demonstrated that both OA isoforms are expressed at all stages with increasing levels of expression as the osteoblasts terminally differentiate. Densitometric analysis of OA expression showed that both the mature and native isoforms increased by ~250%, in the third week of primary culture compared to the first week (Fig. 2A). These data suggest an important role for the mature OA isoform in regulating the terminal differentiation of osteoblasts in culture.

We next examined the expression pattern of OA in different cellular compartments. Here we collected total primary osteoblast cell lysates that had been cultured for 3 weeks before termination. Fractionation of total cell lysates followed by Western blot analysis showed that the mature and native/immature OA isoforms were absent in the nuclear fraction, thereby confirming that OA protein has no nuclear localization sequence (Fig. 2B). The mature OA isoform was highly expressed in the cytoplasmic fraction compared to the native/immature OA isoform (Fig. 2B). The mature OA isoform was expressed in the membranous fraction while the native/immature OA isoform was absent from that fraction (Fig. 2B). Next, we examined whether the mature isoform of OA is secreted by osteoblasts into the conditioned medium. Primary osteoblasts were cultured for three weeks, and 24 h prior to harvesting; the cells were switched to serum free medium. This conditioned media and the corresponding cell layers were then analyzed for OA expression. Western blot analysis showed that the mature OA isoform of 115 kDa was highly expressed in the cell lysates and secreted into the conditioned medium (Fig. 2C). Although the native/immature OA isoform of 65 kDa showed lower levels of expression in the osteoblast cell lysate, it was absent from the conditioned medium. These data suggest that the mature OA isoform is secreted; however, the

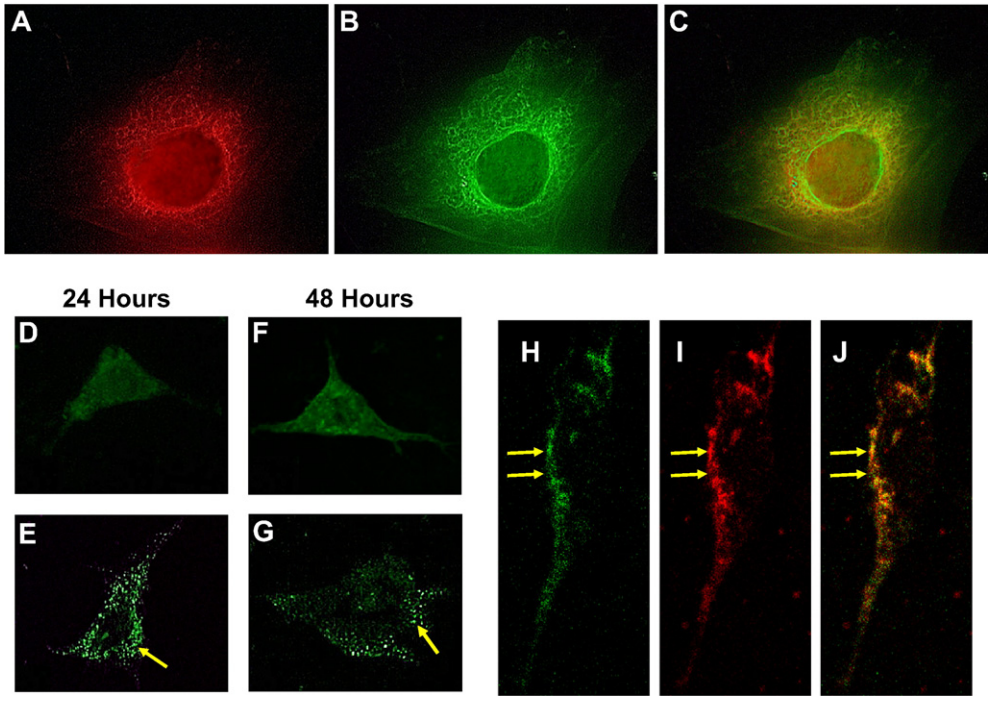

Fig. 3 – Localization of osteoactivin into osteoblasts. (A–C) Immunofluorescent localization of OA in osteoblasts. Primary rat osteoblasts were cultured for two days, fixed and dual stained with anti-OA antibody (A, red signal), or rough ER (rER) marker (B, green signal) and visualized using epifluorescent microscopy. OA is localized to the peri-nuclear area specifically in the rough ER as demonstrated by co-localization between OA and rER markers (C, yellow signal). (D–G) Transient overexpression/localization of OA in osteoblasts. Primary osteoblasts were transfected with CMV-GFP (D and F) or CMV-GFP-OA (E and G) constructs. Cells were visualized at 24 h (D and E) and 48 h (F and G) using confocal laser scanning microscopy (Magnification = 1500×). Note that CMV-GFP showed diffuse signal throughout the cell at both time points examined, while cells expressing CMV-GFP-OA showed OA in vesicular-like structures localized to the perinuclear cytoplasm at 24 h post-transfection (E) and toward the cell periphery at 48 h post-transfection (G). (H–J) Immunofluorescent dual staining in primary osteoblasts labeled with anti-OA antibody (H, green signal) and DiD plasma membrane dye (I, red signal). Photomicrographs were captured using confocal laser scanning microscope. Note the co-localization of OA signal with member dye (J, yellow signal).

native OA isoform is restricted to the cytoplasm, probably within different cellular compartments (see below).

Localization and trafficking of OA in osteoblasts

From the data provided above, it is clear that OA is expressed and secreted by osteoblasts. In order to examine intracellular localization of OA within osteoblast cellular compartments, we performed immunofluorescent analysis. Primary osteoblasts were cultured for three days, then fixed and stained with anti-OA antibody (Ab-551) (red signal). In order to examine whether OA is co-localized with secretory organelles, a rough endoplasmic reticulum (rER) marker was used (green signal). OA was found to be co-localized with the rER marker, suggesting that the protein is processed through the secretory pathway (Fig. 3A–C). These data are consistent with previous data on Pmel-17, another family member with similar pattern of localization [35]. To further visually confirm the intracellular localization of OA in osteoblasts, we transfected primary osteoblasts with a vector expressing a green-fluorescent protein (GFP)-tagged-OA protein under the control of the cytomegalovirus (CMV) promoter. Cells transfected with a GFP-only vector served as non-specific controls (CMV-EV) (Fig. 3D–G). At 24 h following transfection, OA was localized in a punctuated, vesicle-like pattern in the peri-nuclear cytoplasm (Fig. 3E). At 48 h following transfection, the OA expression was localized towards the periphery of the osteoblasts (Fig. 3G). In order to examine whether OA is localized to the plasma membrane, primary osteoblasts transfected with GFP-OA were labeled with DiD dye, a lipophilic membrane stain that is weakly fluorescent until incorporated into the plasma membrane [43]. Confocal microscopy revealed co-localization of OA signal with the plasma membrane signal (Fig. 3H–J). Collectively, these data suggest that in osteoblasts, OA is synthesized and processed through the secretory pathway and anchored to the plasma membrane.

Glycosylation of mOA isoform

From the above data, we propose that the mOA isoform is post-translationally modified. To further investigate this possibility, we immunoprecipitated OA protein from primary osteoblasts cultures isolated at 1-, 2- and 3-week. A gel, on which cytoplasmic proteins from primary osteoblasts were separated, stained with the Pro-Q Emerald stain that detects glycoproteins by reacting with periodate-oxidized carbohydrate groups [44] (Fig. 4A). Only the mOA isoform was detected, suggesting that this isoform is heavily glycosylated. Furthermore, its expression is increased as the osteoblasts differentiate, reaching maximum levels at 3 weeks in culture as described previously [1,23].

The above information clearly suggests that the mature, high molecular weight isoform of OA is glycosylated as part of its post-translation modification. Bioinformatic analysis of the OA protein sequence showed that OA is potentially glycosylated by *O*-linked (Supplemental Figure 1C) and *N*-linked glycans [20]. To investigate this possibility, total protein isolated from three week primary osteoblast cultures was first treated with PNGase-F, an enzyme that cleaves all asparagine-linked complexes, hybrid or high mannose oligosaccharides. The treatment reduced the MW of the mOA isoform by approximately 20 kDa to a form migrating at 95 kDa. To analyze the *O*-glycan modification of the OA protein, we then treated these osteoblastic proteins with a combination of different enzymes. The combination of Sialidase and *O*-glycosidase were used to remove all Ser/Thr-linked (*O*-linked) Gal-(b1–3)-GalNAc-(a1) and all sialic acid substituted Gal-(b1–3)-GalNAc-(a1), and the addition of β-galactosidase and glucosaminidase were used to assist in the de-glycosylation of larger *O*-linked structures. Our data showed that the mOA isoform was reduced by only 15 kDa to a form migrating at approximately 100 kDa. A combination of the PNGase-F and the *O*-glycan de-glycosylation enzymes reduced the apparent molecular weight of the mOA isoform only slightly more than either did alone, to approximately 90 kDa (Fig. 4B). As

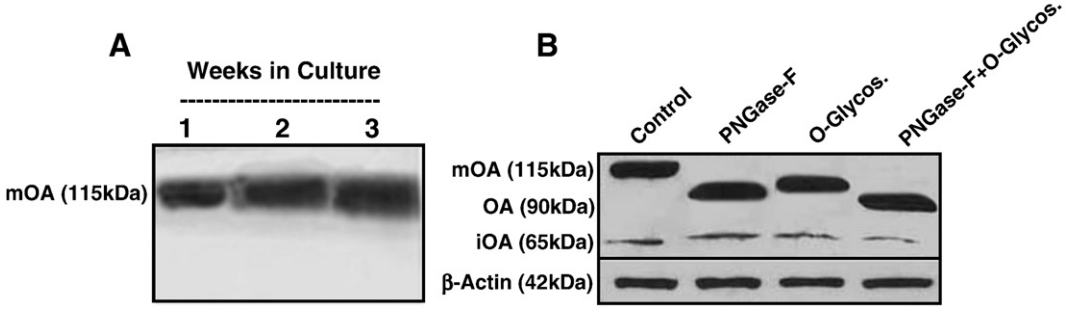

Fig. 4 – Glycosylation of OA in osteoblasts. (A and B) Mature/secreted OA isoform is glycosylated. (A) Primary osteoblasts were cultured and terminated after 1-, 2- and 3-weeks; 50 μg total protein from cell lysates were immunoprecipitated with OA antibody (OA-551), the immunoprecipitates were subjected to SDS-PAGE. The gel was then fixed and stained for glycoproteins with the Pro-Q Emerald 300 gel stain kit. The gel showed only the glycosylated OA isoform at 115 kDa. (B) Primary osteoblasts were cultured for 3 weeks and 20 μg total protein from cell lysates were treated with enzymes to remove N-linked glycoconjugates using PNGase or O-linked glycoconjugates using O-glycosidase as described in the methods. Immunoblot showed a decrease in molecular weight (MW) of the glycosylated OA isoform to 90 kDa with PNGase treatment and to approximately 95 kDa with O-glycosidase treatment. Combined treatment of PNGase with O-glycosidase also decreased the MW of the glycosylated OA isoform to approximately 90 kDa. In all treatment conditions with the different enzymes, the MW of the native/immature OA isoform was not affected. β actin was used as a loading control.

expected, in all cases, the migration of the immature isoform of OA (iOA) was not affected. These results confirm that the mOA protein is modified by a combination of *N*- and *O*-linked glycans.

Regulation of OA glycosylation by retinoic acid and tunicamycin

It has been reported that retinoic acid (RA) treatment alters the glycosylation of alkaline phosphatase in neuronal cell lines [45] and that the treatment with the antibiotic tunicamycin (TM) blocks the first step in glycoprotein synthesis, thus inhibiting the formation of *N*-glycans linked glycoproteins [46]. For our purpose, we were interested in examining whether RA treatment alters the nature of the mOA isoform in osteoblasts. Primary osteoblast cultures were treated with either 10^{-6} M RA, 0.25 μg/ml TM or the combination of both for 24 h prior termination at day 14 (see below) or day 21 (data not shown). Western blots for alkaline phosphatase (ALP), a marker of differentiating osteoblasts used here as a positive control, and for OA were performed and analyzed (Fig. 5A). RA treatment caused an increase in the amounts of both native (58 kDa; iALP) and glycosylated (67 kDa; mALP) isoforms of ALP, while treatment with TM caused a dramatic decrease in the glycosylated, but not the native isoform of ALP as compared to untreated controls. Treatment with both RA and TM was able to rescue the inhibitory effects of TM on ALP glycosylation (Fig. 5A–C). It is interesting to note that treatment with RA increased only the glycosylated, mOA isoform, treatment with TM blocked the glycosylation of mOA. The combination of both factors rescued the glycosylation of mOA isoform similar to that observed for ALP. Unlike ALP, it is important to note that the iOA isoform was not altered in response to either RA or TM treatment (Fig. 5A, D and E).

Densitometry showed increased expression of the glycosylated mOA isoform by 233% on day 14 (Fig. 5D), and by 198% on day 21 (data not shown), after RA treatment. Expression of the glycosylated OA isoform was inhibited by 89% on day 14 (Fig. 5D), and by 85% on day 21 (data not shown), after TM treatment. The iOA isoform was not affected in response to treatment with RA or TM on day 14 (Fig. 5E) or day 21 (data not shown). The results obtained from day 14 and 21 cultures suggested that the regulation of OA glycosylation, at least by RA and TM treatment, was altered during osteoblast differentiation. These results confirm that the mOA is glycosylated by *N*-glycan modifications.

The effects of RA and TM on OA glycosylation was further determined by radiolabeling newly synthesized and modified OA protein using [^{35}S]-methionine and [^{14}C]-mannose

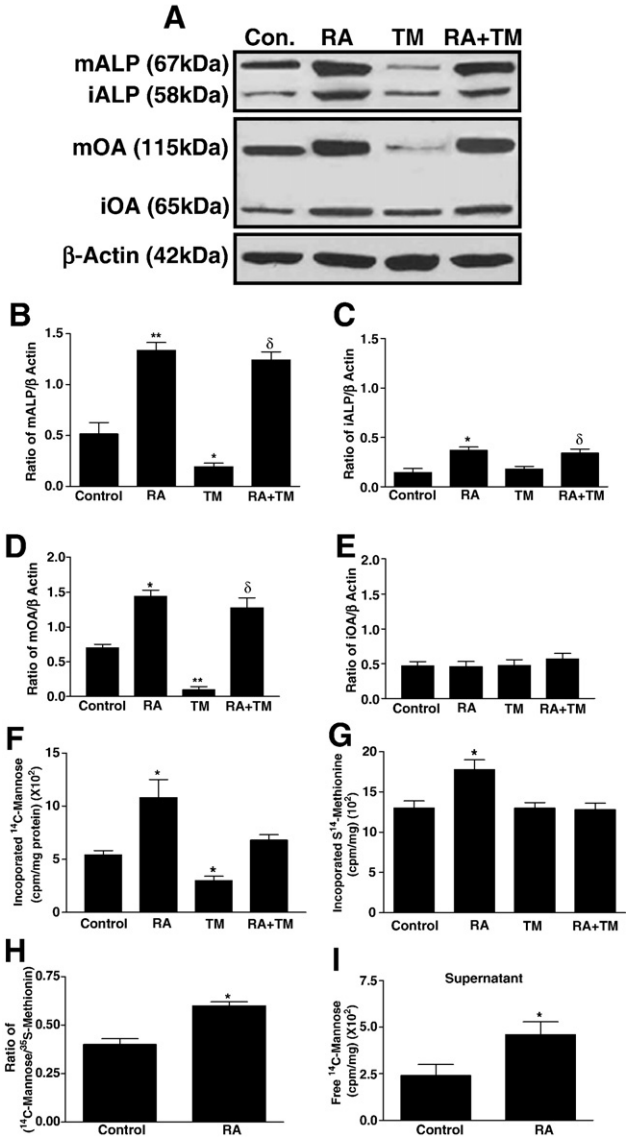

Fig. 5 – Regulation of OA glycosylation. Primary osteoblasts were cultured and treated with 10^{-6} M retinoic acid (RA) in the presence or absence of 1 μg/ml tunicamycin (TM) or TM only for 24 h prior termination on day 14. (A) β actin was used as a loading control. (B and C) Densitometry of 3 immunoblots quantifying the ratio of the glycosylated/mature ALP (B) and native/immature ALP (C) isoforms over β actin. (D and E) Densitometry quantifying the ratio of the glycosylated/mature OA (D) and native/immature OA (E) isoforms over β actin. (F–I) Incorporation of radiolabeled ^{14}C-mannose and ^{35}S-methionnine into OA. Primary osteoblasts were cultured for 3 days then treated with RA, TM, or RA and TM for 24 h. Primary cultures were then switched to serum free medium that have either ^{14}C-mannose (1 μCi/ml) or ^{35}S-methionine (1 μCi/ml) for 12 h before termination. Fifty μg protein aliquots of cell lysates were immunoprecipitated with anti-OA antibody (OA-551). Incorporation of ^{14}C-mannose and ^{35}S-methionine into OA protein were determined via scintillation counting. RA treatment increased ^{14}C-mannose (F) and ^{35}S-methionine (G) incorporation into OA protein, while TM treatment reduced only ^{14}C-mannose incorporation into OA protein (F). Another 50 μg protein aliquot of cell lysates were immunoprecipitated with OA antibody and incubated with PNGase for 1 h at 37 °C and the free ^{14}C-mannose in the supernatant was counted. The ratio of ^{14}C-mannose over ^{35}S-methionine incorporation into OA protein and the free released ^{14}C-mannose from OA protein were calculated and showed that RA treatment increased OA protein synthesis and glycosylation (H and I). Bars represent mean + SEM. * = $p<0.05$; ** = $p<0.01$ when compared to untreated controls; δ = $p<0.01$ when compared to TM treated cultures.

incorporation. Primary osteoblast cultures were treated with RA, TM or both, and then radiolabeled as described in the methods section. OA was immunoprecipitated and the radioactivity incorporated into the newly synthesized OA protein was counted. Treatment with RA significantly increased OA protein synthesis and induced a 2-fold increase in mannosylation, as determined by the incorporation of [^{35}S]-methionine and [^{14}C]-mannose, respectively (Fig. 5F and G). TM treatment inhibited ^{14}C mannose incorporation into OA protein by 45% compared to untreated controls. RA countered the effect of TM on OA protein mannosylation to levels similar to the control (Fig. 5F and G). The ratio of [^{14}C]-mannose over [^{35}S]-methionine incorporation was increased in response to RA treatment (Fig. 5H). To further confirm that RA treatment stimulates mannose incorporation into OA protein, immunoprecipitated OA protein-beads were treated with PNGase-F and free [^{14}C]-mannose released into the supernatant was increased by RA treatment compared to untreated controls (Fig. 5I). Collectively, these data clearly suggest that OA protein is heavily glycosylated and its glycosylation can be modulated by RA. However, the mechanism associated with the effect of RA on stimulation of glycosylation requires further investigations.

Blocking the secreted/mature glycosylated OA protein inhibits early osteoblast differentiation and function

To examine whether the secreted, mature, glycosylated, isoform of OA has a role in early osteoblast differentiation, primary osteoblasts cultures were treated with different concentrations of anti-OA antibody (OA-551) (Fig. 6, dose response not shown), every time the medium was changed. Cultures were terminated and stained for alkaline phosphatase (ALP), a marker of early osteoblast differentiation, on day 14 and for nodules formation assessed on day 17. Primary cultures treated with OA-551 showed less ALP staining (Fig. 6Aa) as well as ALP activity (Fig. 6B) when compared to non-immune IgY treated, control cultures.

The percent of ALP positive area fraction was quantified in each treated and untreated condition using computerized software (BioquantOsteo). Anti-OA antibody treated cultures showed a decrease of 67% in percent ALP area fraction compared to untreated controls (Fig. 6Ab). Anti-OA antibody treated cultures showed a significant decrease in nodule formation (Fig. 6Ca), total number of mineralized nodules (Fig. 6Cb) and average nodule size (Fig. 6Cc) when compared to control cultures. These data suggest an important functional role of the secreted/mature glycosylated OA isoform in the regulation of early osteoblast differentiation.

Blocking the secreted/mature glycosylated OA protein inhibits late osteoblast differentiation

To investigate whether the secreted, mature, glycosylated, isoform of OA has a role in terminal osteoblast differentiation and matrix mineralization, primary osteoblasts were cultured and treated with different concentrations of anti-OA antibody (OA-551) and terminated at day 21 for the measurement of late stage osteoblast differentiation markers (Fig. 7). In order to determine whether the effect of OA-551 on late differentiation is due to a direct effect on cell proliferation or on later stages of

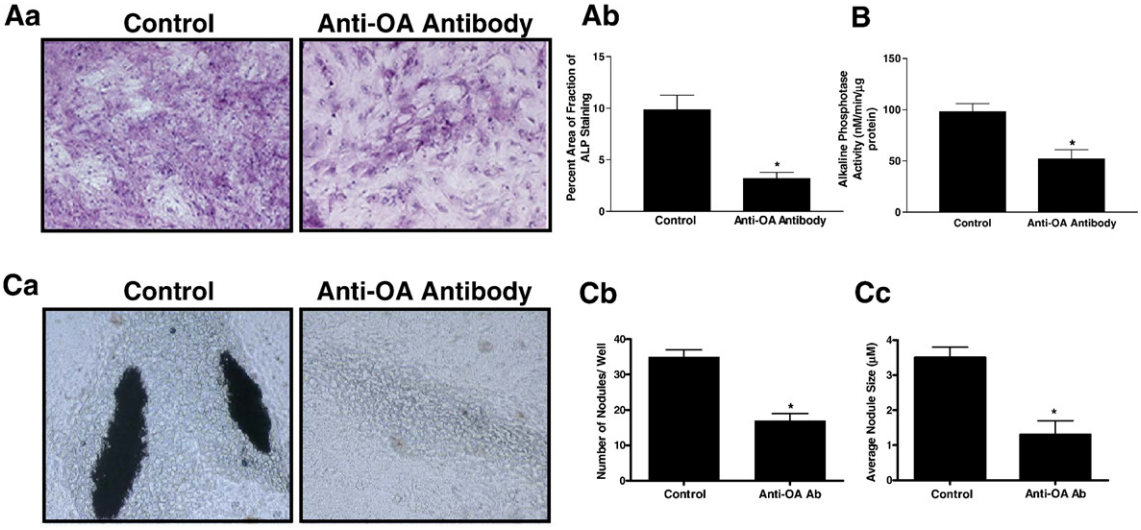

Fig. 6 – Blocking the secreted/mature glycosylated OA protein inhibits osteoblast differentiation. Primary osteoblasts were cultured and treated with anti-OA antibody (OA-551) (20 μg/ml) with every medium change, prior to alkaline phosphatase (ALP) staining, on day 14. (Aa) Photomicrographs showed diminished ALP staining in cultures treated with anti-OA antibody compared to non-immune IgY treated controls. (Ab) Bioquantification of 3 experiments determined that percent area fraction of the field occupied by ALP staining was significantly less with anti-OA antibody treatment. (B) Alkaline phosphatase activity in osteoblasts treated with anti-OA antibody for 14 days, was significantly decreased compared to non-immune IgY treated controls. Measurement of nodule formation in osteoblasts treated with anti-OA antibody on day 17 (Ca and Cb). (Ca) Phase contrast photomicrographs representative of three independent experiments. Nodules are smaller in size and lack minerals in cultures treated with anti-OA antibody when compared to non-immune IgY (control) cultures. (Cb-c) Quantification of three independent experiments for total number of nodules/well and average nodule size. Anti-OA antibody treated cultures showed a significant decrease in total number of nodules (Cb) and average nodule size (Cc) when compared to non-immune IgY (control) cultures. Bars represent mean + SEM. * = $p < 0.05$ when compared to non-immune IgY controls.

differentiation, cultures were treated starting on day 3, when osteoblasts are actively proliferating, with different doses of OA-551, and parallel cultures were treated with the same doses of OA-551 starting on day 11, when the osteoblasts are at the matrix maturation stage. Both cultures were terminated at day 21 for the measurement of late stage osteoblast differentiation markers, such as nodule mineralization by von Kossa staining, calcium deposition, and osteocalcin production (Fig. 7).

When mineralization (percent area fraction of von Kossa staining) was quantified in each treated and condition, we found that anti-OA antibody treatment initiated at either day 3 or day 11 in culture showed a dramatic reduction in areas stained with von Kossa when compared to controls (Fig. 7Aa and Ab for presentation of one dose treatment started at day 3 and terminated at day 21). Anti-OA antibody treated cultures showed a decrease of 70% in percent von Kossa area fraction staining (Fig. 7Ac), as well as a significant decrease in total number of nodules as well as mineralized nodules and nodule size by 54% on day 21 (data not shown) compared to, non-immune IgY treated control cultures. Calcium deposition, a marker also reflecting the matrix mineralization of late stage differentiated osteoblasts, increases in a temporal pattern with osteoblast culture differentiation (Fig. 7B). Treatment with different doses of anti-OA antibody (OA-551), started at day 3 or day 11, significantly inhibited calcium deposition within the osteoblast cultures in a dose response manner (Fig. 7Ca and Cb). In order to examine whether treatment with OA-551 had any effect on cell viability, cultures treated with different doses of anti-OA antibody starting at day 3 or day 11 were terminated at days 5 and 21, respectively, for measurement of

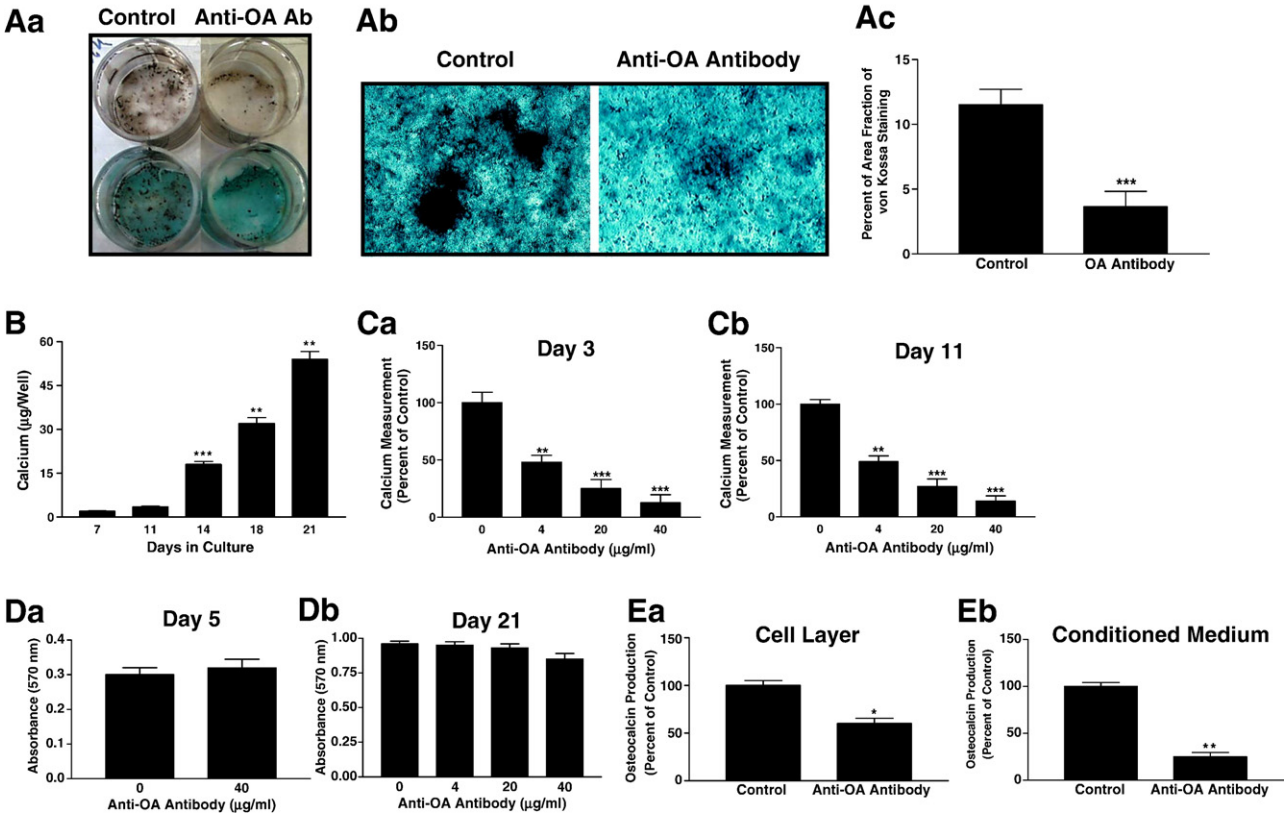

Fig. 7 – Blocking the secreted/mature glycosylated OA protein inhibits osteoblast matrix mineralization. Primary osteoblasts were cultured and treated with anti-OA antibody (OA-551) (20 µg/ml) with every medium change, prior to von Kossa staining on day 21. (A) Photomicrographs of culture wells (Aa) and phase contrast microscopy (Ab) of osteoblasts treated with either non-immune IgY (control) or anti-OA antibody. Von Kossa staining showed a decrease in matrix mineral deposition in cultures treated with anti-OA antibody compared to controls. (Ac) Bioquantification of 3 experiments determined that percent area fraction of the field occupied by von Kossa staining was significantly less with anti-OA antibody treatment when compared to control cultures. (B) Temporal pattern of calcium deposition in normal, untreated primary osteoblast culture matrix over time. Calcium deposition began around day 14 and increased during the period of terminal osteoblast differentiation. (C) Effect of different indicated doses of anti-OA antibody treatment on osteoblast matrix mineralization. Treatment started at different time points, day 3 (Ca) and day 11 (Cb), and terminated at day 21 in culture. (D) MTT-cell viability assay of parallel cultures described in C. Primary osteoblasts were cultured as described in C and treated with anti-OA antibodies starting at day 3 (Da) or day 11 (Db). Both cultures were terminated at day 21 for the measurements of cell viability using the MTT assay as described on the method section. (Ea and Eb) Osteocalcin production in osteoblasts in cell lysates (Ea) and conditioned medium (Eb). Anti-OA antibody treatment significantly reduced osteocalcin production when compared to control cultures. Bars represent mean + SEM of three independent experiments. ** = $p < 0.01$, *** = $p < 0.001$ when compared to non-immune IgY controls or zero in graphs.

cell viability using the MTT assay. OA-551 treatment did not have a significant effect on cell viability when compared to control (non-immune IgY) treated cultures (Fig. 7Da and Db).

Osteocalcin, a secreted marker of terminally differentiated osteoblasts, was also measured in the cell-matrix layer and in the conditioned medium. OA-551 treatment caused a significant decrease in osteocalcin production within the cell-matrix layer and the conditioned medium when compared to control cultures (Fig. 7Ea and Eb). Collectively, these data demonstrate a crucial role for the secreted isoform of OA in the regulation of terminal osteoblast differentiation and matrix mineralization.

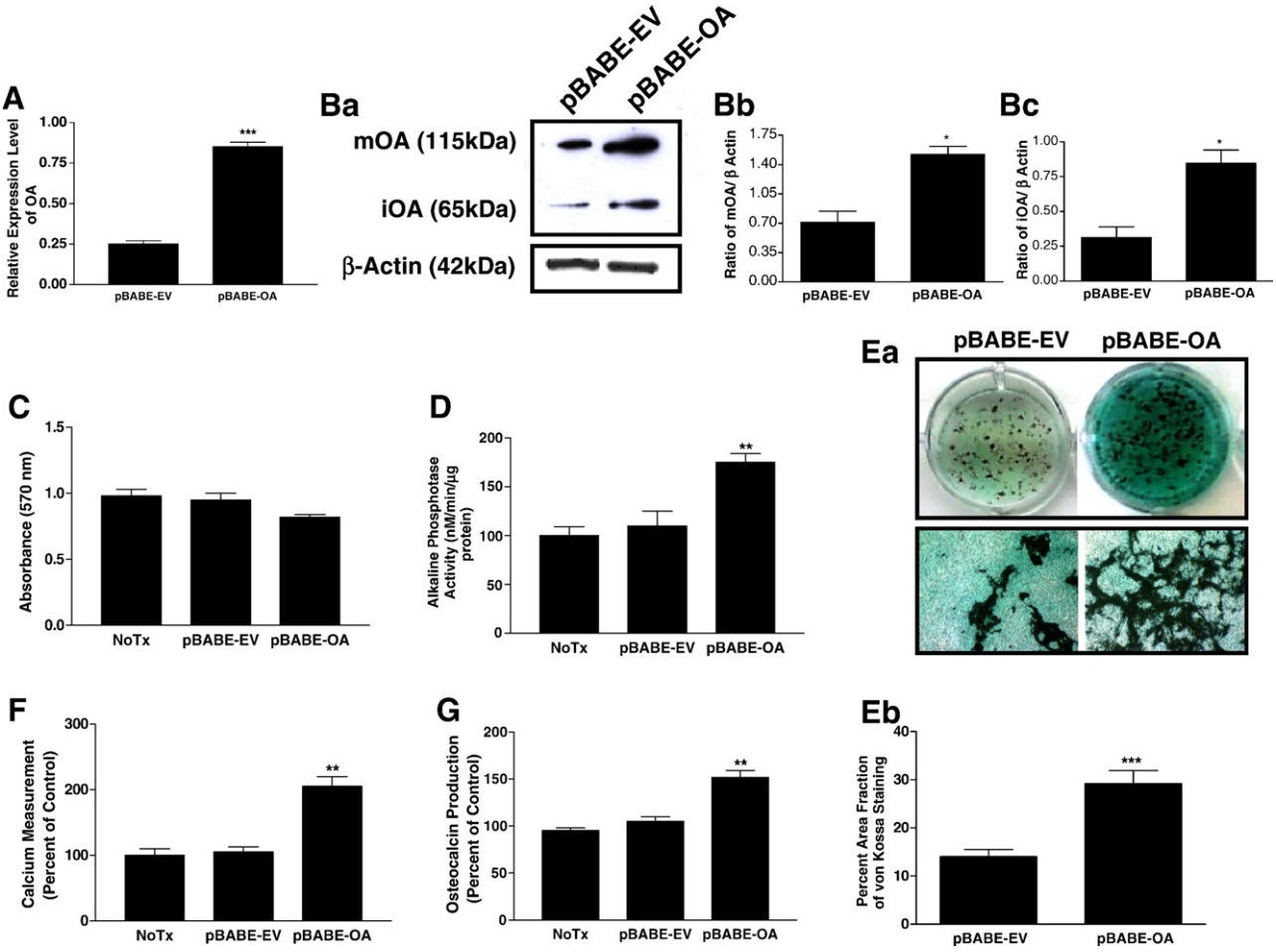

Fig. 8 – Over-expression of OA enhances osteoblast differentiation and function. MC3T3-E1 osteoblast cultures were stably infected with either pBABE-empty retroviral vector (pBABE-EV) or retroviral vector over-expressing osteoactivin (pBABE-OA). Parallel uninfected cultures (No Tx) were used as control. Cultures were terminated at day 5 for the evaluations of OA mRNA (A) and protein (Ba) expression using qPCR and Western blot analysis, respectively. (Bb and Bc) Densitometry of 3 immunoblots quantifying percent of the mature/glycosylated (115 kDa) (Bb), or the immature (65 kDa) isoforms (Bc) of OA protein as a ratio of β actin. Bars represent mean + SEM. * = $p < 0.05$ when compared to cells infected with empty vector. (C) Un-infected (NoTx), stably infected (either pBABE-EV or pBABE-OA) MC3T3-E1 cells were cultured and terminated at day 5 for measurement of cell viability. (D) Un-infected (NoTx) or stably infected (either pBABE-EV or pBABE-OA) MC3T3-E1 cells were cultured and terminated at day 14 for ALP activity measurement. pBABE-OA infected cells showed significant increase in ALP activity when compared to either un-infected (NoTx) or pBABE-EV infected cells. (E–G) Parallel cultures were terminated at day 21 for the measurement of nodule formation and matrix mineralization. (Ea) Photomicrographs (40× magnification) of culture wells (upper panel) and phase contrast (lower panel) of osteoblasts infected with either pBABE-EV or pBABE-OA. Von Kossa staining showed dramatic increase in matrix mineral deposition in cultures over-expressing OA when compared to pBABE-EV infected control cultures. (Eb) Bioquantification of 3 independent experiments determined that percent area fraction of the field occupied by von Kossa staining was significantly increased in cells over-expressing OA (pBABE-OA) compared to control pBABE-EV infected cultures. (F) Calcium deposition was significantly increased in cells infected with pBABE-OA when compared to control cells infected with pBABE-EV or untreated. (G) Osteocalcin production in cell layer of osteoblasts was significantly increased in cultures infected with pBABE-OA when compared to control cultures infected with pBABE-EV or untreated control (NoTx). Bars represent mean + SEM of three independent experiments. ** = $p < 0.01$, when compared to either NoTx or pBABE-EV. *** = $p < 0.001$ when compared to pBABE-EV.

Over-expression of OA enhances osteoblast differentiation and function

We next examined gain-of-function of OA on osteoblast differentiation and function. For this experiment, we utilized the retrovirus pBABE system to overexpress OA in osteoblasts using the MC3T3-E1 osteoblast-like cell line. RetroMax® retrovirus vector system is based on the pCL vector system developed by Naviauz and colleagues [47]. Cells were infected with either pBABE empty vector (pBABE-EV) used as control or pBABE vector over-expressing OA protein (pBABE-OA). Stabely pBABE-OA infected cells demonstrated overexpression of both OA transcript and protein by approximately 2.5-fold (Fig. 8A and Ba). Densitometric analysis of Westerm blots of the OA protein showed that pBABE-OA infected cells over-expressed the mature isoform of OA by approximately 2-fold and the native isoform of OA by approximately 3-fold (Fig. 8Bb and Bc) compared to control (pBABE-EV). We then first examined whether overexpression of OA alters osteoblast proliferation and viability. There was no significant difference between the pBABE-OA and the pBABE-EV cells compared to control (Fig. 8C). Next, we tested the effect of OA overexpression on early (alkaline phosphatase, ALP activity) and late (nodule mineralization, calcium deposition and osteocalcin production) osteoblast differentiation markers. pBABE-OA cells exhibited a significant increases in ALP activity when compared to pBABE-EV and uninfected controls (Fig. 8D). Nodule mineralization as measured by von Kossa staining showed that pBABE-OA cells formed a significantly greater number of mineralized nodules compared to the pBABE-EV control cells (Fig. 8Ea and Eb). Overexpression of OA caused a significant increase in calcium deposition (Fig. 8F) and osteocalcin production (Fig. 8G). Collectively, these data suggest that overexpression of OA stimulates osteoblast differentiation and function.

The OA mutant mouse displays defective osteoblast differentiation ex vivo

A natural point mutation in the osteoactivin mouse gene in which a single nucleotide change introduced a stop codon leading to the generation of a truncated OA protein of only 150 amino acids was originally identified by our collaborators [8] (Fig. 9A). The OA mutant mice develop pigmentary glaucoma [7] and demonstrate enhanced macrophage function [25]. Although the OA mutant mice are fertile and develop normally, we were interested in examining the ability of

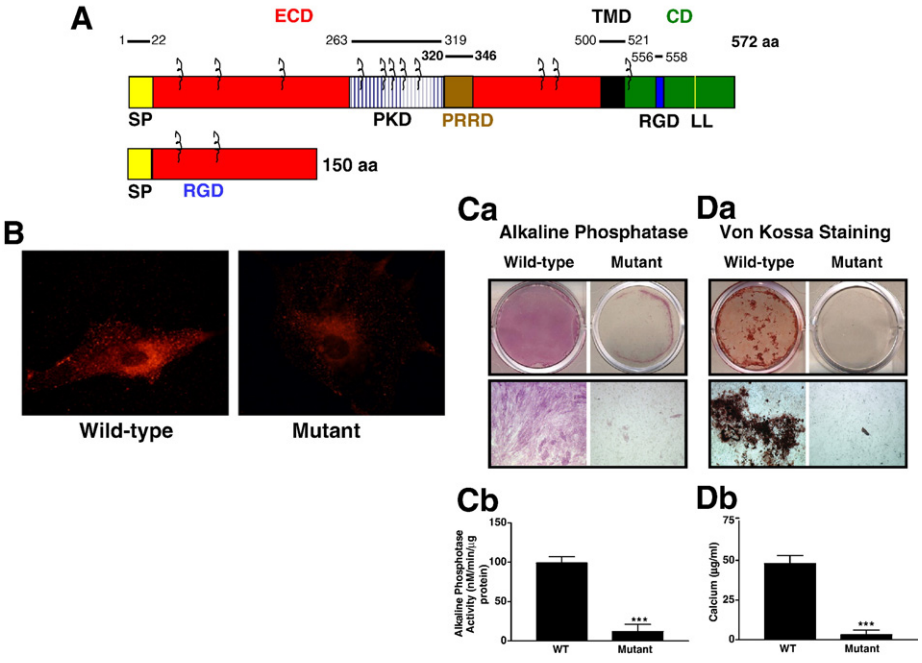

Fig. 9 – Defective differentiation in OA mutant osteoblasts. A. Schematic representation of the wild-type OA (top) and the naturally occurring mutant OA (bottom) proteins. The mutant OA is generated by a premature stop codon mutation. B. Immunofluorescent localization of OA in normal (wild-type) and OA mutant osteoblasts. Primary osteoblasts were isolated from normal and OA mutant mice, cultured for three days and stained with anti-OA antibody (OA-35) (red signal). Note the vesicular localization of OA in wild-type osteoblasts in both perinuclear and peripheral area of the cytoplasm, while in OA mutant osteoblasts, OA is only localized to the perinuclear areas. (C) Bone marrow mesenchymal stem cells from normal and OA mutant mice were harvested as described in the method sections, cultured for 14 days and stained for alkaline phosphatase (ALP) and measured activity. Photomicrographs of culture plate (Ca) or measurement of ALP activity (Cb). Mutant osteoblast cultures demonstrated a significant decrease in ALP staining and activity compared to wild -type cultures. (D) Bone marrow mesenchymal stem cells from normal and OA mutant mice were cultured for 28 days and stained with von Kossa for mineral deposition. Phase contrast pictures (upper panel) (Da) or calcium measurement (Db). Note lack of mineralization in cultures of mutant compared to wild-type osteoblasts.

osteoblasts isolated from OA mutant mice to differentiate ex vivo. We first confirmed that the OA mutant mice have the point mutation (data not shown). We then evaluated the expression of the OA protein in primary cultures of osteoblasts established from OA mutant and wild-type mice, using Western blot analysis. Using an anti-OA antibody directed at the N-terminal end of the mature OA protein (OA-35), we could not unambiguously detect an OA protein in the mutant osteoblasts (data not shown). We next analyzed the localization of the OA protein in osteoblasts isolated from OA mutant and wild-type mice. Immunofluorescent analysis of OA protein in mutant osteoblasts using the OA-35 antibody showed that the OA protein was strictly localized to the perinuclear cytoplasmic regions, in contrast to wild-type osteoblasts where OA is also found in punctuated vesicle-like structures localized toward the peripheral cytoplasmic compartment (Fig. 9B). These data suggest that the OA protein is not processed normally and is retained within the ER/Golgi in OA mutant osteoblasts. We next examined OA mutant osteoblasts for their ability to differentiate ex vivo. Bone marrow mesenchymal stem cells were isolated from OA mutant and wild-type 8–week old mice and cultured for 14 and 21 days. ALP staining and activity and calcium deposition were measured as markers of early and late osteoblast differentiation and function, respectively. Both ALP activity and calcium deposition were dramatically reduced in OA mutant compared to wild-type osteoblasts (Fig. 9C and D). These data suggest that OA acts as a positive regulator of osteoblastogenesis ex vivo and that OA has a cell autonomous defect in osteoblast differentiation and function.

Discussion

In the present study, we demonstrated that OA protein is expressed and secreted by osteoblasts in vitro. We also showed that osteoblasts expressed both the immature and mature/glycosylated isoforms of OA and that retinoic acid and tunicamycin can modulate the glycosylation of OA in osteoblasts and that osteoblasts secret the mature/glycosylated isoform of OA. This isoform of OA plays a role in osteoblast differentiation and function. Osteoblasts that express a mutant isoform of OA are defective in their differentiation ex vivo suggesting that OA has a positive cell autonomous effect on osteoblastogenesis in vivo.

Osteoactivin (OA) was initially identified as a transmembrane type I glycoprotein non-melanoma b (gpnmb) in low metastatic melanoma cell lines [4]. OA was identified by several investigators in different species, mouse OA was identified in dendritic cells, termed cell heparan sulfate proteoglycan integrin dependant ligand (DC-HIL). Human OA was identified in hematopoietic cells, termed growth factor inducible neurokinin (HGFIN). In bone, our group was the first to identify OA [1] in animal model of osteopetrosis. OA has not yet been designated to specific family of proteins; however, it has high homology to Pmel-17/gp100, a melanocyte specific protein [48] and quail neuroretina, QNR-71 protein, all of which are type I transmembrane glycoprotein with secreted isoforms [42,49].

In this study, we characterized OA protein processing in osteoblasts and examined its role in osteoblast differentiation and function using gain- and loss-of-function approaches. Data presented in this study showed that OA protein is expressed by primary osteoblasts in culture. The temporal pattern of OA expression during osteoblast differentiation in culture was examined and showed that OA expression was increased as osteoblast terminally differentiated. OA expression has been associated with differentiating cells of various types such as chondrocytes [50], denderitic cells [10], macrophages [34], myocytes [30], and osteoclasts (un-published observations and personal communication with Dr. Mary Nakamura, University of California, San Francisco). Taken together, our data and others suggested that OA plays a general role in cell differentiation.

Examination of OA protein sequence using different bioinformatic resources revealed that OA protein is a type I transmembrane glycoprotein with a signal peptide, and three main domains, a long extracellular (luminal) domain (amino acids 23–500), short transmembrane domain (amino acids 501–521) and the cytoplasmic domain (amino acids 522–572). Previous reports suggest that the signal peptide sequence of other OA homology proteins such as; Pmel-17, determine their entry into the secretory pathway [51].

Within the extracellular domain, there are three subdomains; the RGD domain, the polycystic kidney disease-like domain (PKD) domain, and the proline rich repeat domain (PRRD). The RGD domain is only present in the N-terminus of moue and human but not in the rat OA. This domain has been shown to mediate the attachment of smooth blood vessel endothelial cell line (SVEC) via heparan sulfate proteoglycan-dependent mechanism [10]. The PKD domain has an immunoglobulin-like folding structure [52]. This domain is suggested to mediate protein–protein interaction and protein–carbohydrate interaction [53]. The PRR domain has been linked to *O*-linked glycans of Pmel-17 and the formation of melanocyte organelle fibers [37]. To date, there is no studies been reported on the functions of different domains of OA in bone cells, however, recent studies using mutant OA lacking the PKD or the PRR domains and tagged to the IgG-Fc demonstrated that the PDK domain with lesser extent, the PRR domain, are required for the inhibitory effect of OA, on T cell activation [9].

The transmembrane domain of OA again has no clear function and yet to be determined by our group in osteoblasts, however, it seems that it plays a role in anchoring OA protein within the cell membrane. It is interesting however; that the cytoplasmic domain of OA consists of RGD domain only in the mouse and rat sequence, and the C-terminal domain also contains di-leucine motif in all species examined. This sequence has been reported to be important for protein sorting of the rough endoplasmic reticulum, in two high homology proteins to OA, Pmel-17 and QNR-71 and several other proteins [38,42,54,55].

Studying the subcellular localization of OA and its processing will shed some light on its mechanism of action on bone cells. For this purpose, our cell fractionation results clearly showed that OA has two isoforms in bone cells. Both protein isoforms are made within the cytosol and only the mature isoform is localized to the membranous fraction. It is important to note that this fraction not only includes the plasma membrane but also all membrane proteins within different cellular compartments. We also presented immunofluorescent data where

EGFP-tagged-OA in osteoblasts, these data suggested that the protein is made, and localized in vesicular-, endosomal-like structures within the first 24 h of expression, then; the protein moves toward the periphery and either anchores itself to the plasma membrane or become secreted. Similar to our results, Shikano et al., showed that in denderitic cells, OA is localized to vesicle-like structures perinuclear as well as small vesicles scattered toward the periphery and present at low levels on the cell surface [10]. Another study showed that subcellular localization of EGFP-tagged OA transfected into COS7 and HEK293 cells. OA was localized to vesicular, endosomal like structures and this localization was dispersed into the ER when the Golgi network was disrupted with BFA treatment. Brefeldin A (BFA) is a fungal metabolite that block cytosolic coat protein complex (COP) function within Golgi compartment [56,57]. Additional supporting evidence on OA subcellular localization came from the co-localization of OA with β-COP, cytosolic coat protein complex, a protein that is associated with membranous structure of the Golgi complex [58–60]. Subcellular localization of Pmel-17 in melanocytes is extensively studied by different groups [38,61–63]. Pmel-17 accumulates in both multivesicular bodies (MVB) and in early endosomal like organelles involved in protein sorting to the endocytic and secretory pathways, respectively. Our group is in the process of characterizing in details the subcellular localization of OA and its relationship to osteoblast function.

In this study, we also found that OA protein is heavily glycosylated by *N*-linked and *O*-linked glycans and that the secreted isoform of OA is the glycosylated/mature isoform of the protein. The fact that treatment of osteoblastic proteins with different enzymes that modulate the *N*- and *O*- glycans of OA did not trim all of the sugar modifications of the protein, i.e. we were unable to reduce the MW of OA protein to its native (65 kDa) size. This is could be due to the time and or the amount of enzymes used in this study. Different patterns of OA glycosylation were suggested based on the cell type examined. Shikano et al., showed discrepancies in the molecular weight of mouse OA between its native size in XS52 denderitic cells and its recombinant form expressed in COS-1 cells and suggested that this heterogeneity in OA proteins may be produced as a result of differential *N*- and/or *O*-glycosylation [10]. Similar observations are recently reported using the same de-glycosylation enzymes to modulate the sugar modifications of Pmel-17 in melanocytes [35]. The same group reported that Pmel17 is glycosylated differently in the Golgi and sorted through the secretory pathway. Using glycosylation-deficient mutant cells revealed that Pmel-17 lacking the correct addition of sialic acid and galactose loses the ability to from fibrils, a critical component of melanin biosynthesis [35].

We went further to examine the regulation of the *N*-glycan modification of OA protein in osteoblasts and found that retinoic acid (RA), and tunicamycin (TM), treatments stimulates *N*-mannose incorporation and inhibits *N*-glycans of OA, respectively. RA has been reported to affect protein glycosylation in vitro [64] and in vivo [65,66]. In this study, we showed that treatment of primary osteoblasts with RA increases the glycosylation of the mature isoform of OA and this treatment was associated with increased osteoblast differentiation and function marked by increased ALP activity and matrix mineralization (data not shown). Tunicamycin on the other hand, inhibited the glycosylation of the mature OA isoform and this treatment was also correlated with decreased osteoblast differentiation and function, demonstrated by dramatic reduction of differentiation markers such as; ALP activity and calcium deposition (data not shown). Collectively, these results probably reflect an overall modulation of osteoblast differentiation and function due to modulation of OA glycosylation. However, we cannot exclude the possibility that other glycoproteins in osteoblasts such as, ALP and bone morphogenetic proteins [45,67], may also be modified by the treatment with RA and TM.

The role of the secreted, glycosylated isoform of OA in osteoblast differentiation was evident by the effect of anti-OA antibody treatment in osteoblast cultures. Treatment with anti-OA antibody (OA-551) neutralizes the constitutively produced OA by osteoblasts and showed a dramatic decrease in markers of osteoblast differentiation and function in a dose-dependent manner. Recent studies by our laboratory also showed that transfection of OA-551 into osteoblasts significantly reduced osteoblast differentiation and function [20]. It is important to note that OA-551 antibody was raised against a sequence that spans the sorting signal in the c-terminal domain of OA. This suggests that the antibody blocks the sorting, processing and secretion of OA by osteoblasts and ultimately inhibits osteoblast differentiation and function.

The effect of OA-551 treatment on osteoblast differentiation was supported by the effect of gain-of-function of OA in osteoblasts. Over-expression of OA stimulated markers of osteoblast differentiation and function. These data suggest that OA has a crucial function in the regulation of osteoblast differentiation.

The role of OA in osteoblast differentiation and function in vivo was further investigated using a mouse model with a natural mutation in the OA gene causing a premature stop codon that results in the generation of a truncated OA protein [7,8,32,33]. These mice develop an eye phenotype with iris pigmentary dispersion (IPD) and iris stromal atrophy (ISA) (see below for other phenotypes). They also have increased macrophage function [34]. In this study we examined the ability of bone marrow mesenchymal stem cells isolated from OA mutant mice to differentiate into osteoblasts. We found that osteoblast differentiation was impaired in OA mutant compared to wild-type mice. These data suggest that OA acts as a positive regulator of osteoblastogenesis in vivo. Further characterization of the skeletal phenotype of these mice warrants further investigations. The fact that mutant OA mice produce truncated OA protein that is lacking most of the structural domains suggested that the truncated OA is retained within the endoplasmic reticulum (ER) resulting in defective protein processing, glycosylation, trafficking, and secretion in osteoblasts. Increased trafficking of OA to lysosomes and/or proteasomal degradation could also be occurring in OA mutant osteoblasts. However, these speculations require further investigation. Similar findings were demonstrated in the mouse *sliver* mutant where Pmel-17, a family member to OA, is truncated at the C-terminal domain, leading to protein retention in the ER and defective protein processing, glycosylation, trafficking and function in melanocytes resulting in a defective coat color and depletion of hair follicle melanocytes with age [68,69]. Another example has been reported for the human Crouzon craniosynostosis syndrome

involving aberrant development of the craniofacial skeleton [70], is associated with an FGFR2 mutation that results in ER retention, diminished glycosylation and increased degradation in osteoblasts [71].

From the data presented here we showed that loss-of-function experiment (using anti-OA antibody) and gain-of-function experiment using the retroviral system either inhibit or stimulate osteoblast differentiation and function, respectively. These data delineate an autocrine/paracrine function of OA during osteoblast differentiation. The mechanism by which OA regulates osteoblast differentiation and function could be direct by regulating specific signaling pathways that modulate specific target genes important for osteoblast development and function. Another possibility is that secreted OA form acts as a matrix protein and binds to integrins and the integrin co-receptor, syndecan, and this interaction induces signaling pathways important for osteoblast differentiation and function [15], and unpublished observation by our group. Another possibility could be explained by the recent study reported by our group where OA acts as a downstream mediator of BMP-2 function in osteoblasts. Loss-of-function or gain-of-function of OA could either decrease or enhance the function of endogenous BMP-2 produced by osteoblasts, respectively [23]. Understanding the various autocrine/paracrine functions of OA on different bone cell types (osteoblasts and mesenchymal stem cells) will enhance our understanding of the role of OA as a positive regulator of bone remodeling and could be the basis for exciting new prophylactic, diagnostic and therapeutic applications in the management of bone loss-associated diseases.

Collectively, in this study we showed that OA acts as anabolic factor where it regulates osteoblast differentiation and function in vitro. Further studies are warranted to determine the mechanism by which OA regulates osteoblast differentiation and bone formation.

Acknowledgments

This research work was supported by grants from the National Institute of Arthritis and Musculoskeletal and Skin Diseases (AR48892) to F.F.S., National Institute of Health and Grant from the Department of Health, State of Pennsylvania to S.M.A. The authors will also like to thank Dr. Archana Sanjay for her comments and suggestions on the experimental design.

Appendix A. Supplementary data

Supplementary data associated with this article can be found, in the online version, at doi:10.1016/j.yexcr.2008.02.006.

REFERENCES

[1] F.F. Safadi, J. Xu, S.L. Smock, M.C. Rico, T.A. Owen, S.N. Popoff, Cloning and characterization of osteoactivin, a novel cDNA expressed in osteoblasts, J. Cell. Biochem. 84 (2001) 12–26.
[2] C.T. Kuan, K. Wakiya, J.M. Dowell, J.E. Herndon II, D.A. Reardon, M.W. Graner, G.J. Riggins, C.J. Wikstrand, D.D. Bigner, Glycoprotein nonmetastatic melanoma protein B, a potential molecular therapeutic target in patients with glioblastoma multiforme, Clin. Cancer Res. 12 (2006) 1970–1982.
[3] K.F. Tse, M. Jeffers, V.A. Pollack, D.A. McCabe, M.L. Shadish, N.V. Khramtsov, C.S. Hackett, S.G. Shenoy, B. Kuang, F.L. Boldog, J.R. MacDougall, L. Rastelli, J. Herrmann, M. Gallo, G. Gazit-Bornstein, P.D. Senter, D.L. Meyer, H.S. Lichenstein, W.J. LaRochelle, CR011, a fully human monoclonal antibody-auristatin E conjugate, for the treatment of melanoma, Clin. Cancer Res. 12 (2006) 1373–1382.
[4] M.A. Weterman, N. Ajubi, I.M. van Dinter, W.G. Degen, G.N. van Muijen, D.J. Ruitter, H.P. Bloemers, nmb, a novel gene, is expressed in low-metastatic human melanoma cell lines and xenografts, Int. J. Cancer 60 (1995) 73–81.
[5] I. Okamoto, C. Pirker, M. Bilban, W. Berger, D. Losert, C. Marosi, O.A. Haas, K. Wolff, H. Pehamberger, Seven novel and stable translocations associated with oncogenic gene expression in malignant melanoma, Neoplasia 7 (2005) 303–311.
[6] V.A. Pollack, E. Alvarez, K.F. Tse, M.Y. Torgov, S. Xie, S.G. Shenoy, J.R. MacDougall, S. Arrol, H. Zhong, R.W. Gerwien, W.F. Hahne, P.D. Senter, M.E. Jeffers, H.S. Lichenstein, W.J. LaRochelle, Treatment parameters modulating regression of human melanoma xenografts by an antibody-drug conjugate (CR011-vcMMAE) targeting GPNMB, Cancer Chemother. Pharmacol. 60 (2007) 423–435.
[7] M.G. Anderson, R.T. Libby, M. Mao, I.M. Cosma, L.A. Wilson, R.S. Smith, S.W. John, Genetic context determines susceptibility to intraocular pressure elevation in a mouse pigmentary glaucoma, BMC Biol. 4 (2006) 20.
[8] M.G. Anderson, R.S. Smith, N.L. Hawes, A. Zabaleta, B. Chang, J.L. Wiggs, S.W. John, Mutations in genes encoding melanosomal proteins cause pigmentary glaucoma in DBA/2J mice, Nat. Genet. 30 (2002) 81–85.
[9] J.S. Chung, K. Sato, I.I. Dougherty, P.D. Cruz Jr., K. Ariizumi, DC-HIL is a negative regulator of T lymphocyte activation, Blood 109 (2007) 4320–4327.
[10] S. Shikano, M. Bonkobara, P.K. Zukas, K. Ariizumi, Molecular cloning of a dendritic cell-associated transmembrane protein, DC-HIL, that promotes RGD-dependent adhesion of endothelial cells through recognition of heparan sulfate proteoglycans, J. Biol. Chem. 276 (2001) 8125–8134.
[11] P.S. Bandari, J. Qian, G. Yehia, D.D. Joshi, P.B. Maloof, J. Potian, H.S. Oh, P. Gascon, J.S. Harrison, P. Rameshwar, Hematopoietic growth factor inducible neurokinin-1 type: a transmembrane protein that is similar to neurokinin 1 interacts with substance P, Regul. Pept. 111 (2003) 169–178.
[12] G.J. Adema, A.J. de Boer, A.M. Vogel, W.A. Loenen, C.G. Figdor, Molecular characterization of the melanocyte lineage-specific antigen gp100, J. Biol. Chem. 269 (1994) 20126–20133.
[13] R.E. Boissy, B. Richmond, M. Huizing, A. Helip-Wooley, Y. Zhao, A. Koshoffer, W.A. Gahl, Melanocyte-specific proteins are aberrantly trafficked in melanocytes of Hermansky–Pudlak syndrome-type 3, Am. J. Pathol. 166 (2005) 231–240.
[14] E. Jager, M. Maeurer, H. Hohn, J. Karbach, D. Jager, Z. Zidianakis, A. Bakhshandeh-Bath, J. Orth, C. Neukirch, A. Necker, T.E. Reichert, A. Knuth, Clonal expansion of Melan A-specific cytotoxic T lymphocytes in a melanoma patient responding to continued immunization with melanoma-associated peptides, Int. J. Cancer 86 (2000) 538–547.
[15] L.S. Kierstead, E. Ranieri, W. Olson, V. Brusic, J. Sidney, A. Sette, Y.L. Kasamon, C.L. Slingluff Jr., J.M. Kirkwood, W.J. Storkus, gp100/pmel17 and tyrosinase encode multiple epitopes recognized by Th1-type CD4+T cells, Br. J. Cancer 85 (2001) 1738–1745.
[16] M. Sensi, S. Pellegatta, C. Vegetti, G. Nicolini, G. Parmiani, A. Anichini, Identification of a novel gp100/pMel17 peptide presented by HLA-A*6801 and recognized on human melanoma by cytolytic T cell clones, Tissue Antigens 59 (2002) 273–279.

[17] J.C. Valencia, T. Hoashi, J.M. Pawelek, F. Solano, V.J. Hearing, Pmel17: controversial indeed but critical to melanocyte function, Pigment Cell Res. 19 (2006) 250–252 author reply 253–7.
[18] S.N. Wagner, C. Wagner, T. Schultewolter, M. Goos, Analysis of Pmel17/gp100 expression in primary human tissue specimens: implications for melanoma immuno- and gene-therapy, Cancer Immunol. Immunother. 44 (1997) 239–247.
[19] J.F. Berson, D.C. Harper, D. Tenza, G. Raposo, M.S. Marks, Pmel17 initiates premelanosome morphogenesis within multivesicular bodies, Mol. Biol. Cell 12 (2001) 3451–3464.
[20] A.A. Selim, S.M. Abdelmagid, R.A. Kanaan, S.L. Smock, T.A. Owen, S.N. Popoff, F.F. Safadi, Anti-osteoactivin antibody inhibits osteoblast differentiation and function in vitro, Crit. Rev. Eukaryot. Gene Expr. 13 (2003) 265–275.
[21] J.N. Rich, Q. Shi, M. Hjelmeland, T.J. Cummings, C.T. Kuan, D.D. Bigner, C.M. Counter, X.F. Wang, Bone-related genes expressed in advanced malignancies induce invasion and metastasis in a genetically defined human cancer model, J. Biol. Chem. 278 (2003) 15951–15957.
[22] T.A. Owen, S.L. Smock, S. Prakash, L. Pinder, D. Brees, D. Krull, T.A. Castleberry, Y.C. Clancy, S.C. Marks Jr., F.F. Safadi, S.N. Popoff, Identification and characterization of the genes encoding human and mouse osteoactivin, Crit. Rev. Eukaryot. Gene Expr. 13 (2003) 205–220.
[23] S.M. Abdelmagid, M.F. Barbe, I. Arango-Hisijara, T.A. Owen, S.N. Popoff, F.F. Safadi, Osteoactivin acts as downstream mediator of BMP-2 effects on osteoblast function, J. Cell. Physiol. 210 (2007) 26–37.
[24] V. Lennerz, M. Fatho, C. Gentilini, R.A. Frye, A. Lifke, D. Ferel, C. Wolfel, C. Huber, T. Wolfel, The response of autologous T cells to a human melanoma is dominated by mutated neoantigens, Proc. Natl. Acad. Sci. U. S. A. 102 (2005) 16013–16018.
[25] J.S. Mo, M.G. Anderson, M. Gregory, R.S. Smith, O.V. Savinova, D.V. Serreze, B.R. Ksander, J.W. Streilein, S.W. John, By altering ocular immune privilege, bone marrow-derived cells pathogenically contribute to DBA/2J pigmentary glaucoma, J. Exp. Med. 197 (2003) 1335–1344.
[26] J.H. Ahn, Y. Lee, C. Jeon, S.J. Lee, B.H. Lee, K.D. Choi, Y.S. Bae, Identification of the genes differentially expressed in human dendritic cell subsets by cDNA subtraction and microarray analysis, Blood 100 (2002) 1742–1754.
[27] B. Haralanova-Ilieva, G. Ramadori, T. Armbrust, Expression of osteoactivin in rat and human liver and isolated rat liver cells, J. Hepatol. 42 (2005) 565–572.
[28] M. Onaga, A. Ido, S. Hasuike, H. Uto, A. Moriuchi, K. Nagata, T. Hori, K. Hayash, H. Tsubouchi, Osteoactivin expressed during cirrhosis development in rats fed a choline-deficient, L-amino acid-defined diet, accelerates motility of hepatoma cells, J. Hepatol. 39 (2003) 779–785.
[29] H. Abe, H. Uto, Y. Takami, Y. Takahama, S. Hasuike, M. Kodama, K. Nagata, A. Moriuchi, M. Numata, A. Ido, H. Tsubouchi, Transgenic expression of osteoactivin in the liver attenuates hepatic fibrosis in rats, Biochem. Biophys. Res. Commun. 356 (2007) 610–615.
[30] T. Ogawa, T. Nikawa, H. Furochi, M. Kosyoji, K. Hirasaka, N. Suzue, K. Sairyo, S. Nakano, T. Yamaoka, M. Itakura, K. Kishi, N. Yasui, Osteoactivin upregulates expression of MMP-3 and MMP-9 in fibroblasts infiltrated into denervated skeletal muscle in mice, Am. J. Physiol., Cell Physiol. 289 (2005) C697–C707.
[31] A. Nakamura, A. Ishii, C. Ohata, T. Komurasaki, Early induction of osteoactivin expression in rat renal tubular epithelial cells after unilateral ureteral obstruction, Exp. Toxicol. Pathol. 59 (2007) 53–59.
[32] M.G. Anderson, R.S. Smith, O.V. Savinova, N.L. Hawes, B. Chang, A. Zabaleta, R. Wilpan, J.R. Heckenlively, M. Davisson, S.W. John, Genetic modification of glaucoma associated phenotypes between AKXD-28/Ty and DBA/2J mice, BMC Genet. 2 (2001) 1.
[33] C. Ott, D. Iwanciw, A. Graness, K. Giehl, M. Goppelt-Struebe, Modulation of the expression of connective tissue growth factor by alterations of the cytoskeleton, J. Biol. Chem. 278 (2003) 44305–44311.
[34] V.M. Ripoll, K.M. Irvine, T. Ravasi, M.J. Sweet, D.A. Hume, Gpnmb is induced in macrophages by IFN-gamma and lipopolysaccharide and acts as a feedback regulator of proinflammatory responses, J. Immunol. 178 (2007) 6557–6566.
[35] J.C. Valencia, F. Rouzaud, S. Julien, K.G. Chen, T. Passeron, Y. Yamaguchi, M. Abu-Asab, M. Tsokos, G.E. Costin, H. Yamaguchi, L.M. Jenkins, K. Nagashima, E. Appella, V.J. Hearing, Sialylated core 1 *O*-glycans influence the sorting of Pmel17/gp100 and determine its capacity to form fibrils, J. Biol. Chem. 282 (2007) 11266–11280.
[36] K.S. Lau, E.A. Partridge, A. Grigorian, C.I. Silvescu, V.N. Reinhold, M. Demetriou, J.W. Dennis, Complex *N*-glycan number and degree of branching cooperate to regulate cell proliferation and differentiation, Cell 129 (2007) 123–134.
[37] T. Hoashi, J. Muller, W.D. Vieira, F. Rouzaud, K. Kikuchi, K. Tamaki, V.J. Hearing, The repeat domain of the melanosomal matrix protein PMEL17/GP100 is required for the formation of organellar fibers, J. Biol. Chem. 281 (2006) 21198–21208.
[38] A.C. Theos, S.T. Truschel, D. Tenza, I. Hurbain, D.C. Harper, J.F. Berson, P.C. Thomas, G. Raposo, M.S. Marks, A lumenal domain-dependent pathway for sorting to intralumenal vesicles of multivesicular endosomes involved in organelle morphogenesis, Dev. Cell 10 (2006) 343–354.
[39] D. J. Morre, D. M. Morre, Preparation of mammalian plasma membranes by aqueous two-phase partition. Biotechniques 7 (1989) 946–8, 950–4, 956–8.
[40] K. Zerivitz, G. Akusjarvi, An improved nuclear extract preparation method, Gene Anal. Tech. 6 (1989) 101–109.
[41] A. Rezania, K.E. Healy, Integrin subunits responsible for adhesion of human osteoblast-like cells to biomimetic peptide surfaces, J. Orthop. Res. 17 (1999) 615–623.
[42] R. Le Borgne, N. Planque, P. Martin, F. Dewitte, S. Saule, B. Hoflack, The AP-3-dependent targeting of the melanosomal glycoprotein QNR-71 requires a di-leucine-based sorting signal, J. Cell Sci. 114 (2001) 2831–2841.
[43] B. Khoobehi, G.A. Peyman, Fluorescent labeling of blood cells for evaluation of retinal and choroidal circulation, Ophthalmic Surg. Lasers 30 (1999) 140–145.
[44] B. Schulenberg, J.M. Beechem, W.F. Patton, Mapping glycosylation changes related to cancer using the Multiplexed Proteomics technology: a protein differential display approach, J. Chromatogr. B Analyt. Technol. Biomed. Life Sci. 793 (2003) 127–139.
[45] W.H. Mueller, D. Kleefeld, B. Khattab, J.D. Meissner, R.J. Scheibe, Effects of retinoic acid on *N*-glycosylation and mRNA stability of the liver/bone/kidney alkaline phosphatase in neuronal cells, J. Cell. Physiol. 182 (2000) 50–61.
[46] N. Takahashi, A. Iwahori, T.R. Breitman, T. Fukui, Tunicamycin in combination with retinoic acid synergistically inhibits cell growth while decreasing palmitoylation and enhancing retinoylation of proteins in the human breast cancer cell line MCF-7, Oncol. Res. 9 (1997) 527–533.
[47] R.K. Naviaux, E. Costanzi, M. Haas, I.M. Verma, The pCL vector system: rapid production of helper-free, high-titer, recombinant retroviruses, J. Virol. 70 (1996) 5701–5705.
[48] T. Kobayashi, K. Urabe, S.J. Orlow, K. Higashi, G. Imokawa, B.S. Kwon, B. Potterf, V.J. Hearing, The Pmel 17/silver locus protein. Characterization and investigation of its melanogenic function, J. Biol. Chem. 269 (1994) 29198–29205.
[49] N. Turque, F. Denhez, P. Martin, N. Planque, M. Bailly, A. Begue, D. Stehelin, S. Saule, Characterization of a new melanocyte-specific gene (QNR-71) expressed in v-myc-transformed quail neuroretina, Embo J. 15 (1996) 3338–3350.

[50] C.G. James, C.T. Appleton, V. Ulici, T.M. Underhill, F. Beier, Microarray analyses of gene expression during chondrocyte differentiation identifies novel regulators of hypertrophy, Mol. Biol. Cell 16 (2005) 5316–5333.
[51] G.A. Maresh, J.S. Marken, M. Neubauer, A. Aruffo, I. Hellstrom, K.E. Hellstrom, H. Marquardt, Cloning and expression of the gene for the melanoma-associated ME20 antigen, DNA Cell Biol. 13 (1994) 87–95.
[52] A.M. Scanu, C. Edelstein, Apolipoprotein(a): structural and functional consequences of mutations in kringle type 10 (or kringle 4–37), Clin. Genet. 46 (1994) 42–45.
[53] M.S. Scheffers, H. Le, P. van der Bent, W. Leonhard, F. Prins, L. Spruit, M.H. Breuning, E. de Heer, D.J. Peters, Distinct subcellular expression of endogenous polycystin-2 in the plasma membrane and Golgi apparatus of MDCK cells, Hum. Mol. Genet. 11 (2002) 59–67.
[54] R. Piccirillo, I. Palmisano, G. Innamorati, P. Bagnato, D. Altimare, M.V. Schiaffino, An unconventional dileucine-based motif and a novel cytosolic motif are required for the lysosomal and melanosomal targeting of OA1, J. Cell Sci. 119 (2006) 2003–2014.
[55] V. Setaluri, Sorting and targeting of melanosomal membrane proteins: signals, pathways, and mechanisms, Pigment Cell Res. 13 (2000) 128–134.
[56] D. Bachner, D. Schroder, G. Gross, mRNA expression of the murine glycoprotein (transmembrane) nmb (Gpnmb) gene is linked to the developing retinal pigment epithelium and iris, Brain Res. Gene Expr. Patterns 1 (2002) 159–165.
[57] S.Y. Bednarek, M. Ravazzola, M. Hosobuchi, M. Amherdt, A. Perrelet, R. Schekman, L. Orci, COPI- and COPII-coated vesicles bud directly from the endoplasmic reticulum in yeast, Cell 83 (1995) 1183–1196.
[58] G. Griffiths, R. Pepperkok, J.K. Locker, T.E. Kreis, Immunocytochemical localization of beta-COP to the ER–Golgi boundary and the TGN, J. Cell Sci. 108 (Pt 8) (1995) 2839–2856.
[59] J. Scheel, R. Pepperkok, M. Lowe, G. Griffiths, T.E. Kreis, Dissociation of coatomer from membranes is required for brefeldin A-induced transfer of Golgi enzymes to the endoplasmic reticulum, J. Cell Biol. 137 (1997) 319–333.
[60] L.C. Hendricks, M. McCaffery, G.E. Palade, M.G. Farquhar, Disruption of endoplasmic reticulum to Golgi transport leads to the accumulation of large aggregates containing beta-COP in pancreatic acinar cells, Mol. Biol. Cell 4 (1993) 413–424.
[61] J.C. Valencia, H. Watabe, A. Chi, F. Rouzaud, K.G. Chen, W.D. Vieira, K. Takahashi, Y. Yamaguchi, W. Berens, K. Nagashima, J. Shabanowitz, D.F. Hunt, E. Appella, V.J. Hearing, Sorting of Pmel17 to melanosomes through the plasma membrane by AP1 and AP2: evidence for the polarized nature of melanocytes, J. Cell Sci. 119 (2006) 1080–1091.
[62] G. Raposo, D. Tenza, D.M. Murphy, J.F. Berson, M.S. Marks, Distinct protein sorting and localization to premelanosomes, melanosomes, and lysosomes in pigmented melanocytic cells, J. Cell Biol. 152 (2001) 809–824.
[63] S.R. Setty, D. Tenza, S.T. Truschel, E. Chou, E.V. Sviderskaya, A.C. Theos, M.L. Lamoreux, S.M. Di Pietro, M. Starcevic, D.C. Bennett, E.C. Dell'Angelica, G. Raposo, M.S. Marks, BLOC-1 is required for cargo-specific sorting from vacuolar early endosomes toward lysosome-related organelles, Mol. Biol. Cell 18 (2007) 768–780.
[64] L. De Luca, G. Wolf, Vitamin A and mucus secretion. A brief review of the effect of vitamin A on the biosynthesis of glycoproteins, Int. Z. Vitaminforsch. 40 (1970) 284–290.
[65] M.J. Kirven, G. Wolf, Synthesis and glycosylation of fibronectin in hepatocytes from vitamin A-deficient rats, Mol. Cell. Biochem. 101 (1991) 101–114.
[66] D. Rimoldi, K.E. Creek, L.M. De Luca, Reduced mannose incorporation into GDP-mannose and dolichol-linked intermediates of *N*-glycosylation in hamster liver during vitamin A deficiency, Mol. Cell. Biochem. 93 (1990) 129–140.
[67] L. Garrigue-Antar, N. Hartigan, K.E. Kadler, Post-translational modification of bone morphogenetic protein-1 is required for secretion and stability of the protein, J. Biol. Chem. 277 (2002) 43327–43334.
[68] A.C. Theos, J.F. Berson, S.C. Theos, K.E. Herman, D.C. Harper, D. Tenza, E.V. Sviderskaya, M.L. Lamoreux, D.C. Bennett, G. Raposo, M.S. Marks, Dual loss of ER export and endocytic signals with altered melanosome morphology in the silver mutation of Pmel17, Mol. Biol. Cell 17 (2006) 3598–3612.
[69] A.C. Theos, S.T. Truschel, G. Raposo, M.S. Marks, The Silver locus product Pmel17/gp100/Silv/ME20: controversial in name and in function, Pigment Cell Res. 18 (2005) 322–336.
[70] K. Mangasarian, Y. Li, A. Mansukhani, C. Basilico, Mutation associated with Crouzon syndrome causes ligand-independent dimerization and activation of FGF receptor-2, J. Cell. Physiol. 172 (1997) 117–125.
[71] N.E. Hatch, M. Hudson, M.L. Seto, M.L. Cunningham, M. Bothwell, Intracellular retention, degradation, and signaling of glycosylation-deficient FGFR2 and craniosynostosis syndrome-associated FGFR2C278F, J. Biol. Chem. 281 (2006) 27292–27305.